Cell Death and Differentiation (2016) 23, 1331–1346

www.nature.com/cdd

NLRP3 regulates a non-canonical platform for caspase-8 activation during epithelial cell apoptosis

H Chung[1,3], A Vilaysane[1,3], A Lau[1], M Stahl[2], V Morampudi[2], A Bondzi-Simpson[1], JM Platnich[1], NA Bracey[1], M-C French[1], PL Beck[1], J Chun[1], BA Vallance[2] and DA Muruve*[,1]

Nod-like receptor, pyrin containing 3 (NLRP3) is characterized primarily as a canonical caspase-1 activating inflammasome in macrophages. NLRP3 is also expressed in the epithelium of the kidney and gut; however, its function remains largely undefined. Primary mouse tubular epithelial cells (TEC) lacking Nlrp3 displayed reduced apoptosis downstream of the tumor necrosis factor (TNF) receptor and CD95. TECs were identified as type II apoptotic cells that activated caspase-8, tBid and mitochondrial apoptosis via caspase-9, responses that were reduced in *Nlrp3*−/− cells. The activation of caspase-8 during extrinsic apoptosis induced by TNFα/cycloheximide (TNFα/CHX) was dependent on adaptor protein apoptosis-associated speck-like protein containing a CARD (ASC) and completely independent of caspase-1 or caspase-11. TECs and primary human proximal tubular epithelial cells (HPTC) did not activate a canonical inflammasome, caspase-1, or IL-1β secretion in response to TNFα/CHX or NLRP3-dependent triggers, such as ATP or nigericin. In cell fractionation studies and by confocal microscopy, NLRP3 colocalized with ASC and caspase-8 in speck-like complexes at the mitochondria during apoptosis. The formation of NLRP3/ASC/caspase-8 specks in response to TNFα/CHX was downstream of TNFR signaling and dependent on potassium efflux. Epithelial ASC specks were present in enteroids undergoing apoptosis and in the injured tubules of wild-type but not *Nlrp3*−/− or *ASC*−/− mice following ureteric unilateral obstruction *in vivo*. These data show that NLRP3 and ASC form a conserved non-canonical platform for caspase-8 activation, independent of the inflammasome that regulates apoptosis within epithelial cells.
Cell Death and Differentiation (2016) **23,** 1331–1346; doi:10.1038/cdd.2016.14; published online 19 February 2016

Nod-like receptor, pyrin containing 3 (NLRP3) is an innate sensor that has been characterized primarily as an inflammasome-forming protein in leukocytes.[1] NLRP3 is activated by a wide range of pathogen/danger-associated molecular patterns to regulate host cellular responses to infection and injury.[1] In the canonical pathway, NLRP3 activation triggers the oligomerization of the adaptor protein apoptosis-associated speck-like protein containing a CARD (ASC) and caspase-1 into a high molecular weight inflammasome that regulates cytokine maturation (IL-1β and IL-18) and pyroptosis.[2] Emerging studies have demonstrated non-canonical NLRP3 inflammasomes that activate alternate caspases such as caspase-8 and caspase-11 in leukocytes and more recently caspase 4/11 in the intestinal epithelium.[3–5]

Caspase-8 is an initiator caspase in the apoptosis pathway activated downstream of death receptors such as tumor necrosis factor receptor (TNFR) and CD95. In type I apoptotic cells, caspase-8 is recruited to the death-inducing signaling complex (DISC) at the plasma membrane where it undergoes autocleavage and acts directly upon the executioner caspase-3 to initiate apoptosis.[6] In type II apoptotic cells, caspase-8 activation at the DISC is inhibited by the caspase-3 inhibitor x-linked inhibitor of apoptosis (XIAP) and cellular FLICE inhibitory protein (cFLIP).[6–8] Type II cells require the mitochondrial pathway to fully initiate the cell death program via caspase-8 activation at the outer mitochondrial membrane that cleaves Bid to tBid.[9] tBid triggers the oligomerization of Bax/Bak, which initiates mitochondrial outer membrane permeabilization, cytochrome *c* release and activation of caspase-9.[6, 10] Initiation of mitochondrial apoptosis also releases SMAC/DIABLO, which inhibits XIAP and enables caspase-3 to further activate caspase-8.[11]

Caspase-8 is also activated downstream of the NLRP3, AIM2 and NLRC4 inflammasomes in response to canonical triggers in macrophages[4,12–14] or downstream of Dectin-1 in dendritic cells.[15–17] The activation of caspase-8 in leukocytes requires ASC and regulates the non-canonical maturation of IL-1β. However in caspase-1/11-deficient macrophages, caspase-8 also regulates apoptosis downstream of AIM2 and NLRP3 inflammasomes.[4,12] The relationship between NLRP3, ASC and caspase-8 activation during apoptosis in the absence of inflammasome activation or in a physiological caspase-1-deficient system has not yet been evaluated.

Epithelial cells have key roles in tissue homeostasis, host defense, immune regulation and regeneration. In the kidney,

[1]Department of Medicine, Snyder Institute for Chronic Diseases, University of Calgary, Calgary, AB, Canada and [2]Department of Pediatrics, Child and Family Research Institute, University of British Columbia, Vancouver, BC, Canada
*Corresponding author: DA Muruve, Department of Medicine, Snyder Institute for Chronic Diseases, University of Calgary, 3280 Hospital Drive NW, Calgary, AB T2N 4Z6, Canada. Tel: +1 403 220 2418; Fax: +1 403 210 3949; E-mail: dmuruve@ucalgary.ca
[3]These authors contributed equally to this work.

Abbreviations: ASC, apoptosis-associated speck-like protein containing a CARD; BMDM, bone marrow-derived macrophages; CHX, cycloheximide; cFLIP, cellular FLICE inhibitory protein; DISC, death-inducing signaling complex; FLICA, FAM-LETD-fmk or FAM-YVAD-fmk; HPTC, primary human proximal tubular epithelial cells; LPS, lipopolysaccharide; MSU, monosodium urate crystals; MTT, 3-(4, 5-dimethylthiazol-2-yl)-2, 5-diphenyltetrazolium bromide; NLRP3, Nod-like receptor, pyrin containing 3; TEC, primary mouse tubular epithelial cells; TNFR, tumor necrosis factor receptor; UUO, unilateral ureteric obstruction; XIAP, x-linked inhibitor of apoptosis

Received 18.6.15; revised 30.12.15; accepted 20.1.16; Edited by M Deshmukh; published online 19.2.16

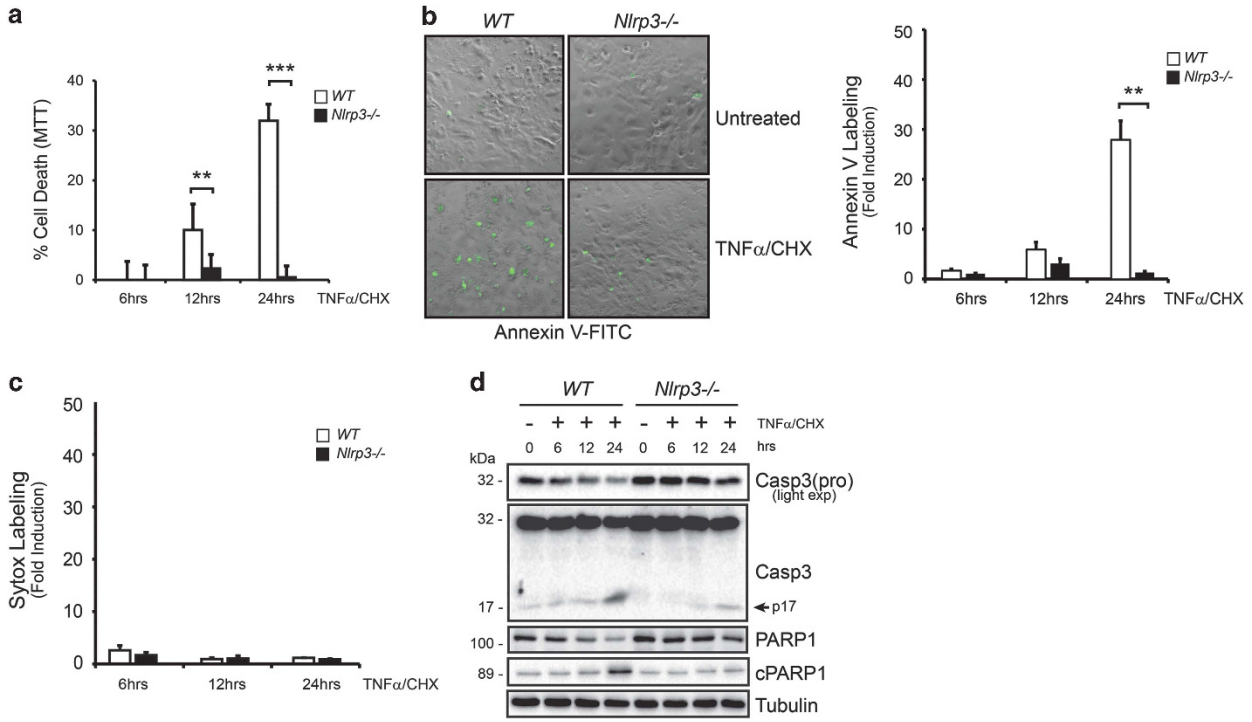

Figure 1 Role of Nlrp3 in tubular epithelial cell apoptosis. (**a**) Cell viability (MTT) assay at 6, 12 and 24 h in wild-type (WT) or *Nlrp3−/−* TECs treated with TNFα (10 ng/ml) and CHX (5 μg/ml) (mean ± S.E.M.; WT *versus Nlrp3−/−*, $^{**}P<0.01$, $n=3$ independent experiments). (**b**) Annexin V immunofluorescence of TECs treated with TNFα/CHX. Images are shown as a brightfield and FITC channel overlay (×10 lens, ×3 zoom). Right panel quantitation of Annexin V positivity in WT or *Nlrp3−/−* TECs treated with TNFα/CHX at 6, 12 and 24 h. (mean ± S.E.M.; WT *versus Nlrp3−/−* $^{**}P<0.01$, $^{***}P<0.001$, $n=3$ independent experiments). (**c**) Sytox orange labeling in WT and *Nlrp3−/−* TECs treated with TNFα/CHX at 6, 12 and 24 h. (**d**) Immunoblotting using antibodies specific for caspase-3 (pro-p32 and cleaved p17), total PARP1 and cleaved PARP1 (cPARP1) in WT and *Nlrp3−/−* TECs induced to undergo apoptosis with TNFα/CHX for 6, 12 and 24 h

tubular epithelial cell apoptosis is a major component of disease that contributes to tubular atrophy and tubulointerstitial fibrosis.[18] The intestinal epithelium lies at the host–microbial interface and is key to maintaining gut homeostasis as well as directing the host response to the gut microbiota and to pathogenic microbes. Inflammasome genes such as NLRP3 and ASC are expressed in both gut and kidney epithelia.[3,19–21] We and others have demonstrated primarily non-canonical and inflammasome-independent roles for NLRP3 in the kidney epithelium and during experimental kidney injury *in vivo*.[20–23] For example, *Nlrp3−/−* mice undergoing renal ischemia/reperfusion or unilateral ureteric obstruction (UUO) display reduced epithelial apoptosis and tubular injury independent of a canonical inflammasome or caspase-1.[20–23] In the intestinal tract, non-canonical NLRP3 regulates IL-18 maturation as well as epithelial cell shedding in response to *Salmonella* infection.[3] Despite these studies, the biology of NLRP3 and other inflammasome-related genes in epithelial cells has yet to be fully elucidated.

Given the increasing evidence of crosstalk between the inflammasome and cell death machinery in the cell, the role of NLRP3 in epithelial cell apoptosis was determined. We show that NLRP3, via ASC, primarily regulates a non-canonical caspase-8-activating platform at the mitochondria that is necessary for epithelial cell death. The activation of caspase-8 by NLRP3 in epithelia occurs independent of canonical NLRP3 triggers, caspase-1, or pro-inflammatory cytokine production.

Results

Nlrp3 is required for apoptosis and caspase-8 activation in epithelial cells. To examine the involvement of Nlrp3 in receptor-mediated epithelial cell apoptosis, primary mouse tubular epithelial cells (TEC) were treated with tumor necrosis factor-*α*/cycloheximide (TNF*α*/CHX) and probed using Annexin V and assessed for viability using the 3-(4, 5-dimethylthiazol-2-yl)-2, 5-diphenyltetrazolium bromide (MTT) assay. At 24 h, *Nlrp3−/−* TECs displayed significantly less cell death as well as reduced surface labeling with Annexin V compared with control wild-type controls (Figures 1a and b). Cell death was due to apoptosis as minimal Sytox orange labeling was observed following TNF*α*/CHX stimulation over 24 h (Figure 1c, Supplementary Figure S1). *Nlrp3−/−* TECs also displayed significantly reduced caspase-3 activation and cleavage of its substrate poly-ADP-ribose polymerase (PARP1) (Figure 1d). Together, these results show that *Nlrp3−/−* TECs exhibit reduced cell death and apoptosis induced by TNF*α*/CHX.

TNF*α*/CHX also induced cleavage of caspase-8 at 24 h in TEC, a response that was significantly diminished in *Nlrp3−/−* cells (Figure 2a). To determine whether Nlrp3 was also required for apoptosis involving the SMAC-dependent/RIP1 pathway[24] or CD95, TECs were stimulated with TNF*α* and the SMAC-mimetic birinapant[25] or an activating CD95 antibody (Jo2). Over 24 h, both TNF*α*/birinapant and anti-CD95 resulted in efficient apoptosis and caspase-8 and

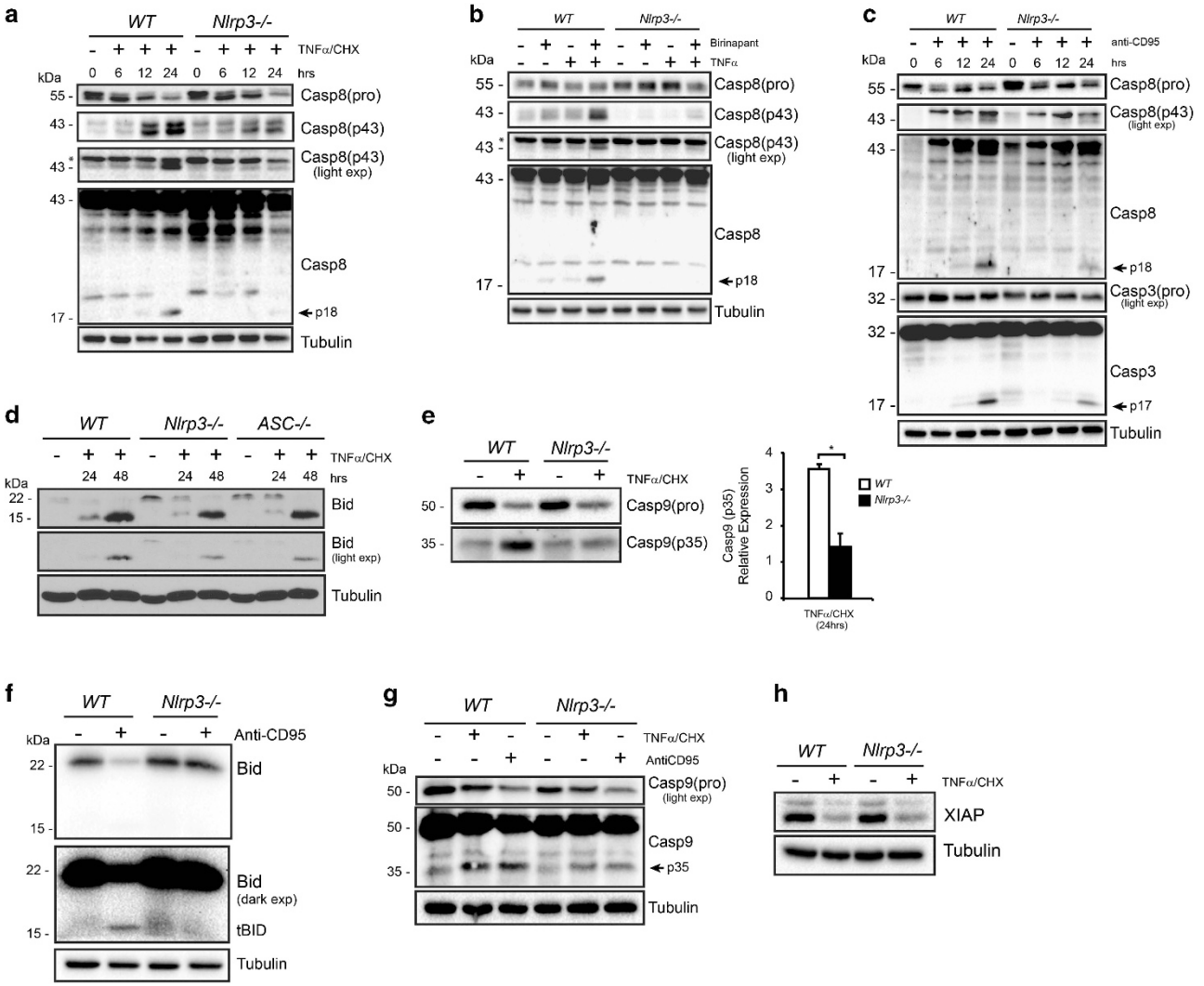

Figure 2 Nlrp3-dependent regulation of death receptor-mediated apoptosis. (**a**) TECs were incubated for the indicated time points with TNFα (10 ng/ml) and CHX (5 μg/ml). Immunoblotting using antibodies specific for caspase-8 (pro), caspase-8 (p41/43) and caspase-8 (p41/43, p18) in wild-type (WT) and *Nlrp3*$-/-$ TECs. Asterisk represents non-specific band. (**b**) Immunoblotting for caspase-8 in WT and *Nlrp3*$-/-$ TECs treated for the indicated times with TNFα (10 ng/ml) and the SMAC-mimetic birinapant (10 μM). (**c**) Immunoblotting for caspase-8 and caspase-3 in WT and *Nlrp3*$-/-$ TECs treated for the indicated times with the activating CD95 antibody (Jo2). (**d**) Immunoblotting for full-length (22 kDa) and cleaved Bid (15 kDa) in WT and *Nlrp3*$-/-$ and *ASC*$-/-$ TECs after TNFα/CHX treatment at 24 and 48 h. (**e**) Immunoblotting for pro-caspase-9 and cleaved caspase-9 (p35) in TECs stimulated with TNFα/CHX. Quantification of caspase-9 normalized to β-tubulin (mean $\pm$ S.D.; TNFα/CHX 24 h, WT *versus* *Nlrp3*$-/-$, $^*P<0.05$, $n=3$ independent experiments). (**f**) Immunoblotting for full-length (22 kDa) and cleaved Bid (15 kDa) in WT and *Nlrp3*$-/-$ TECs after CD95 activation at 24 h. (**g**) Immunoblotting for caspase-9 (pro-p50 and cleaved p35 subunit) in TECs stimulated with TNFα/CHX and CD95 activating antibody at 24 h. (**h**) Immunoblotting for XIAP protein in TNFα/CHX-treated WT and *Nlrp3*$-/-$ TECs at 24 h

caspase-3 activation in wild-type TEC, responses that were significantly impaired in *Nlrp3*$-/-$ cells (Figures 2b and c and Supplementary Figures S2a–c and S3b). Together, these data show that Nlrp3 is required for caspase-8 activation and apoptosis downstream of the TNFR and CD95.

Caspase-8 activation and cell death emerged over 12–24 h, suggesting that TECs represent type II apoptotic cells (Figures 2a–c and Supplementary Figure S2d). Consistent with this premise, TNFα/CHX- and CD95-treated TECs effectively cleaved Bid to truncated Bid (tBid) and activated caspase-9 (Figures 2d–g), responses that were significantly reduced in *Nlrp3*$-/-$ cells. Consistent with their type II cell death phenotype, wild-type and *Nlrp3*$-/-$ TECs express similar levels of DISC genes, including not only TRADD, FADD, TRAF2 and RIP1 (Supplementary Figure S3a) but also the apoptosis inhibitors XIAP and cFLIP (Figure 2h,Supplementary Figure S3a). Furthermore, the SMAC-mimetic birinapant also enhanced CD95-induced apoptosis that was attenuated in *Nlrp3*$-/-$ TECs (Supplementary Figure S3b). In contrast, peritoneal macrophages are type I apoptotic cells that display similar levels of caspase-8 activation in *Nlrp3*$-/-$ and wild-type cells following receptor-mediated cell death as previously described (Supplementary Figure S4a).[26] TECs assumed a type I phenotype and Nlrp3 became dispensable for apoptosis when TNFR and CD95 activation were combined with both

birinapant and CHX to antagonize multiple inhibitory pathways (Supplementary Figure S4b). Finally, fractionation studies were performed comparing primary human proximal tubular epithelial cells (HPTC) and human THP-1 macrophages. In response to TNF*α*/CHX, cytochrome *c* release in the cytoplasm was observed in HPTC but not in THP-1 cells at 24 h (Figure 6a). Together, these data show that Nlrp3 regulates receptor-mediated caspase-8 activation and apoptosis in TECs (type II cells) but not in macrophages (type I cells).

Role of the inflammasome in Nlrp3-mediated caspase-8 activation in TEC. Experiments were next performed to determine whether the regulation of caspase-8 was downstream of the Nlrp3 inflammasome. The activation of the Nlrp3 inflammasome using the canonical agonist nigericin in bone marrow-derived macrophages (BMDM) results in the activation of both caspase-1 and caspase-8 as previously reported[4,13] (Supplementary Figure S5). In the absence of caspase-1 or caspase-11, caspase-8 activation by nigericin is maintained confirming that caspase-8 is a downstream effector of the Nlrp3 inflammasome. Mouse TECs express both Nlrp3 and ASC[21] but compared with BMDM very little caspase-1 as detected by immunoblotting (Figure 3a). In contrast, caspase-11 is expressed in both BMDM and TEC and, as expected, is absent in *caspase-1/11−/−* cells. Caspase-1 was not induced in TECs by TNF*α* or lipopolysaccharide (LPS); however, Nlrp3 was modestly increased by both stimuli (Supplementary Figures S6a and b). Given these data, the possibility existed that, in the absence of caspase-1, Nlrp3 may regulate apoptosis in TECs through the formation of a non-canonical inflammasome involving caspase-8 and/or caspase-11. As caspase-8 has been shown to interact with ASC via its pyrin domain,[4] experiments were performed in *ASC−/−* TEC. In response to TNF*α*/CHX, *ASC−/−* TECs displayed reduced apoptosis, caspase-8 and caspase-3 activation as well as Bid cleavage compared with wild-type cells (Figures 2d and 3b, d and e and Supplementary Figure S1). In contrast, caspase-1 and caspase-11 were dispensable as caspase-8 and caspase-3 activation was intact in *caspase-1/11−/−* TECs (Figures 3c–e and Supplementary Figure S1) and TNF*α*/CHX did not induce caspase-11 cleavage in wild-type or *Nlrp3−/−* TECs at 24 and 48 h (Supplementary Figure S6c). Together, these results exclude caspase-1 and caspase-11 downstream of Nlrp3 in the regulation of caspase-8 in TEC. Rather, these observations suggest that caspase-8 activation may occur through a non-canonical inflammasome involving Nlrp3 and ASC.

Experiments were next performed to evaluate the effect of canonical NLRP3 agonists in TEC. The treatment of LPS-primed TECs with adenosine triphosphate (ATP), monosodium urate crystals (MSU) or nigericin failed to activate caspase-8 (Figure 3f). Similarly, none of the canonical Nlrp3 agonists induced IL-1*β* or IL-18 secretion from TEC, unlike the robust cytokine maturation induced by ATP in BMDM (Figure 3g, Supplementary Figure S6d). Cytokine secretion in TECs was also absent following TNF*α*/CHX treatment, excluding IL-1*β* or IL-18 in the regulation of caspase-8 by Nlrp3. In HPTC that express both caspase-1 and caspase-8, ATP or nigericin failed to activate an inflammasome as demonstrated by caspase-1 or -8 cleavage (Figure 3h). In contrast, THP-1 macrophages process caspase-1 and -8 efficiently in response to nigericin, and HPTC activate caspase-8 but not caspase-1 cleavage in response to TNF*α*/CHX (Figure 3h). LPS or TNF*α* priming had little-to-no effect on caspase-1 or NLRP3 expression levels in HPTC or the ability to respond to canonical Nlrp3 agonists (Supplementary Figure S6e). Thus mouse and human kidney epithelial cells do not readily form canonical inflammasomes or respond to canonical NLRP3 stimuli. Rather, these data suggest that NLRP3 may regulate a non-canonical apoptotic pathway in epithelial cells via ASC and caspase-8.

Nlrp3-dependent caspase-8 activation occurs at the mitochondria. Confocal fluorescence microscopy was used to explore the relationship between Nlrp3, ASC and caspase-8 in tubular epithelial cells. Studies were performed in HPTC as antibodies for Nlrp3, in our hands, perform poorly for immunofluorescence microscopy in TEC. Similar to reports in macrophages and cardiac fibroblasts,[27–29] NLRP3 localized primarily to mitochondria in unstimulated HPTC (Figure 4a). There was no shift in NLRP3 localization between control and TNF*α*/CHX-stimulated cells, although 'speck-like' NLRP3-positive aggregates at the mitochondria could be observed following treatment. ASC was expressed diffusely and did not localize to mitochondria in HPTC at baseline. Following TNF*α*/CHX stimulation, ASC specks became visible that co-localized to mitochondria and with NLRP3 (Figures 4b and c and Supplementary Figure S7a). Unlike macrophages where usually a single ASC speck per cell is formed during inflammasome activation, one to multiple ASC specks per cell could be observed in HPTC undergoing apoptosis. The co-localization of NLRP3 and ASC to mitochondria was specific as isotype controls were negative and no co-staining was observed with the Golgi marker GM130 or the lysosome marker LAMP1 at baseline or following stimulation with TNFα/CHX (Supplementary Figure S7b–d). Furthermore, the formation of ASC specks were confirmed to be occurring in E-cadherin-positive epithelial cells (Supplementary Figure S7e).

Next, to determine the relationship of activated caspase-8 to NLRP3 and ASC specks, a fluorescent-labeled caspase-8 probe FAM-LETD-fmk (FLICA) was employed. Following stimulation with TNF*α*/CHX, a sizable pool of activated caspase-8 but not caspase-1 was detected that co-localized to mitochondria in speck-like structures (Figure 5a, Supplementary Figure S8). Furthermore, NLRP3 and ASC co-localized with caspase-8 within specks in apoptotic HPTC (Figures 5b–d). NLRP3, ASC and caspase-8 also co-localized in HPTC following activation of CD95 (Supplementary Figure S9a). Furthermore, the specificity of ASC/caspase-8 specks were confirmed in *ASC−/−* mouse TECs that demonstrate minimal caspase-8 activation and no ASC staining or speck formation in contrast to wild-type TECs treated with TNF*α*/CHX (Supplementary Figure S9b). In comparison, and consistent with the type I phenotype, TNF*α*/CHX induced active caspase-8 THP-1 macrophages that did not co-localize to NLRP3, ASC or mitochondria (Supplementary Figures S10a and b). Furthermore, no NLRP3 or ASC specks could be observed in

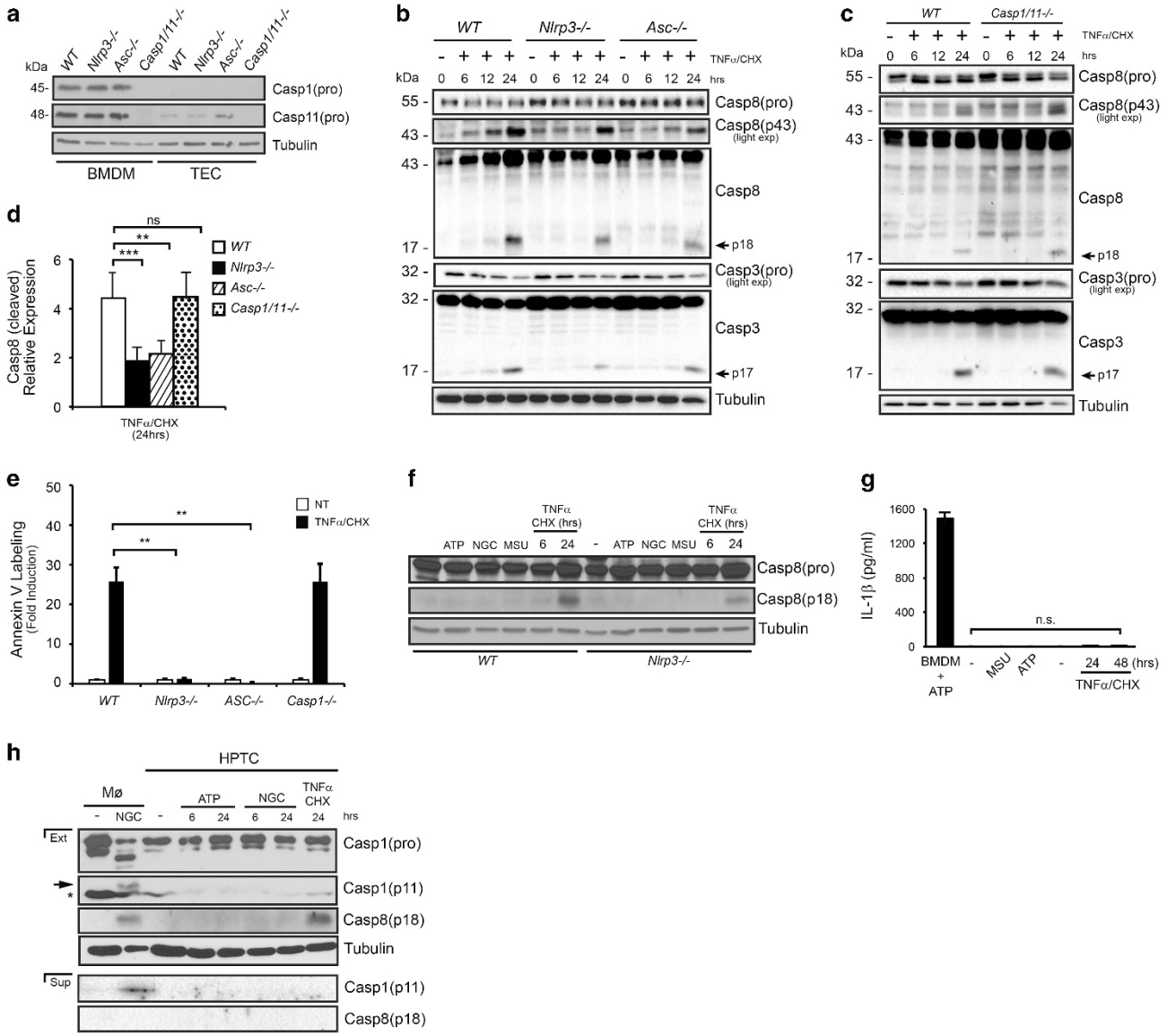

Figure 3 Role of the inflammasome in Nlrp3-mediated caspase-8 activation. (**a**) Immunoblotting for pro-caspase-1 and pro-caspase-11 in wild-type (WT), *Nlrp3*−/−, *ASC*−/− and *casp1/11*−/− BMDMs and TECs. (**b**) Immunoblotting for caspase-8 (using antibodies specific for pro, p41/43 and p41/43/p18 forms) and caspase-3 in WT, *Nlrp3*−/− and *ASC*−/− TECs treated with TNFα (10 ng/ml)/CHX (5 μg/ml) at 6, 12 and 24 h. (**c**) Immunoblotting for caspase-8 and caspase-3 in WT and *casp1/11*−/− TECs treated with TNFα/CHX. (**d**) Quantification of cleaved caspase-8 (p18) normalized to β-tubulin in WT, *Nlrp3*−/−, *ASC*−/− and *casp1/11*−/− TECs at 24 h (mean ± S.D.; WT *versus Nlrp3*−/− ***$P<0.001$ or *ASC*−/− **$P<0.01$; WT *versus Casp1/11*−/−, P=NS; $n=6$ independent experiments). (**e**) Annexin V staining in WT, *Nlrp3*−/−, *ASC*−/− and *casp1/11*−/− TECs treated with TNFα/CHX at 24 h (mean ± S.E.M.; WT *versus Nlrp3*−/− or *ASC*−/−, **$P<0.01$; WT *versus* Casp1/11−/−, P=NS, $n=3$ independent experiments). (**f**) Immunoblotting for pro-caspase-8 and cleaved caspase-8 (p18) in LPS-primed WT and *Nlrp3*−/− TECs treated for 6 h with canonical inflammasome activators ATP (5 mM), nigericin (20 μM) and MSU (100 μg/ml). Cells were also treated with TNFα (10 ng/ml)/CHX (5 μg/ml) for 6 and 24 h as a positive control. (**g**) IL-1β ELISA on WT TECs supernatants after treatment with MSU (100 μg/ml) and ATP (5 mM) for 24 h and TNFα/CHX for 24 and 48 h. LPS-primed BMDM treated with ATP (5 mM) for 1 h was used as a positive control. (**h**) Immunoblotting for pro-caspase-1, cleaved caspase-1 (p11 N-terminal CARD, denoted by arrow. Asterisk is non-specific band) and cleaved caspase-8 in LPS-primed HPTCs extracts and supernatants treated with ATP (5 mM), nigericin (20 μM) and TNFα (10 ng/ml)/CHX (25 ug/ml) for the indicated time points. THP-1 cells treated with 20 μM nigericin for 3 h were utilized as positive controls

THP-1 macrophages undergoing apoptosis (Supplementary Figure S10a). Conversely, the canonical NLRP3 agonist nigericin failed to induce caspase-8 activation, NLRP3 or ASC speck formation in both LPS-primed and unprimed HPTC (Supplementary Figure S11). Together, these results show that death-receptor mediated apoptosis triggers an NLRP3/ASC/caspase-8 complex at the mitochondria in tubular epithelial cells but not in macrophages.

To corroborate the microscopy results, cellular fractionation studies demonstrated significant NLRP3 localization to the mitochondria at baseline in HPTC although significant cytosolic expression was also present (Figures 6a and b). These observations were in stark contrast to the primarily cytoplasmic NLRP3 localization in THP-1 macrophages (Figure 6a). A substantial reduction in the 110-kDa NLRP3 protein occurred in both cellular compartments following

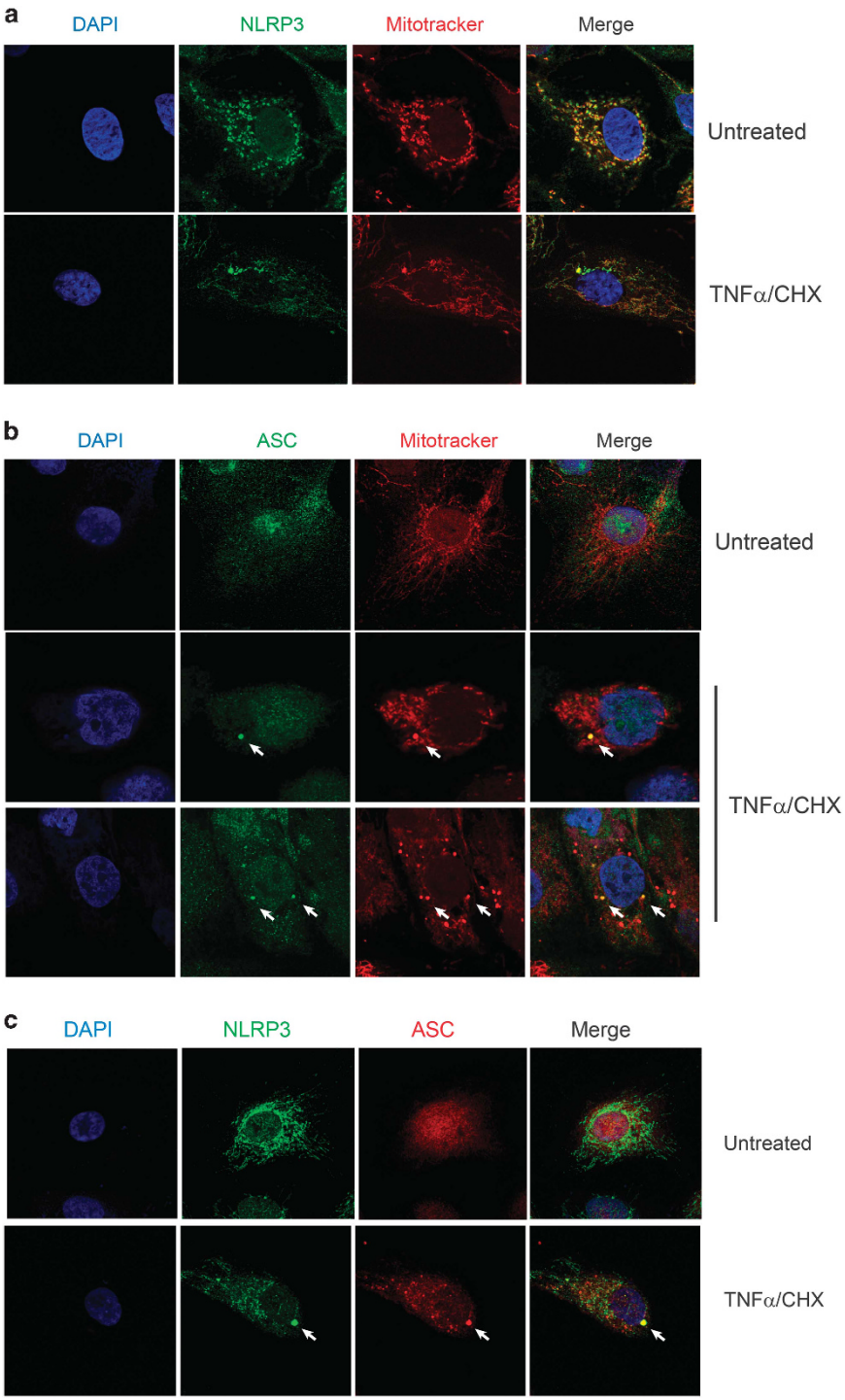

Figure 4 Co-localization of NLRP3 and ASC to mitochondria. Immunofluorescence confocal microscopy. (**a**) Untreated and TNFα (10 ng/ml)/CHX (25 μg/ml)-treated HPTC at 24 h probing for NLRP3 (green) and mitochondria (Mitotracker Red). (**b**) ASC (green) and mitochondria (Mitotracker Red) in untreated and TNFα/CHX-treated HPTC (24 h). Arrows denote ASC co-localization to Mitotracker Red. (**c**) NLRP3 (green) and ASC (red) co-localization in TNFα/CHX-treated HPTC (24 h). Arrows denote ASC and NLRP3 co-localization. All cells were background stained with DAPI (blue) (all ×60 lens, ×3 zoom)

TNFα/CHX stimulation, likely owing to formation of large molecular weight oligomers (Figures 6a and b and Supplementary Figure S12). In contrast to NLRP3, ASC and pro-caspase-8 were restricted primarily to the cytoplasm in unstimulated HPTC. Following TNFα/CHX stimulation, cleaved caspase-8 became enriched in the mitochondrial fraction (Figure 6b). Although the majority of ASC remained cytosolic, ASC monomers and ASC dimers became detectable at the mitochondria in the uncrosslinked and the disuccinimidyl suberate crosslinked fractions, respectively,

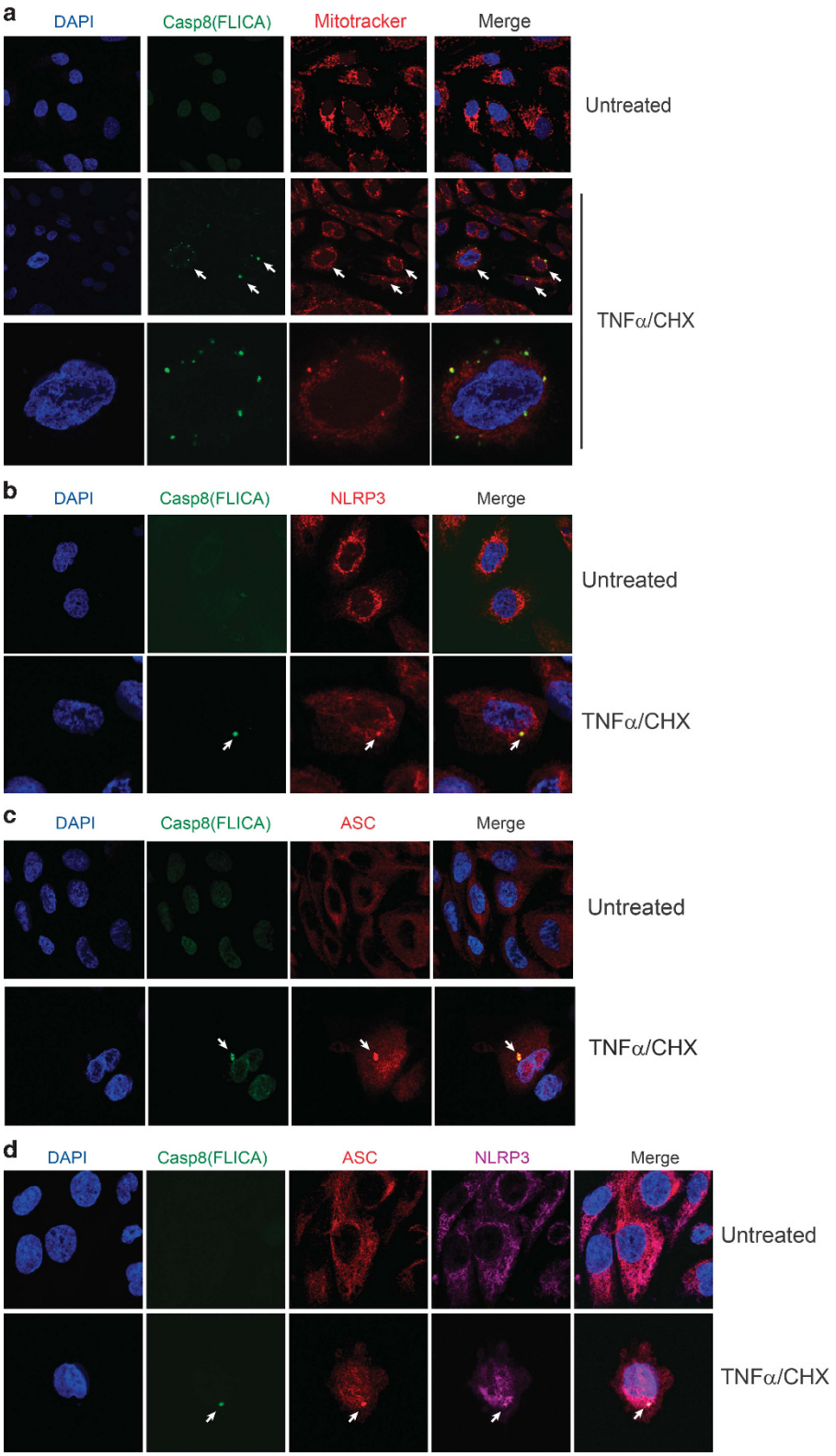

Figure 5 Co-localization of activated caspase-8, NLRP3 and ASC in HPTC. (**a**) Immunofluorescence confocal microscopy. Activated caspase-8 (FLICA, green) and mitochondria (Mitotracker Red) in untreated and TNFα (10 ng/ml)/CHX (25 μg/ml)-treated HPTC (24 h). Upper panels are × 40 lens × 2 zoom, lower panels × 60 lens, × 4 zoom. Arrows denote cells with active caspase-8 co-localizing to mitochondria. Caspase-8 co-localization with (**b**) NLRP3 (red) and (**c**) ASC (red) in HPTC untreated and treated with TNFα/CHX at 24 h. Upper panels × 40 lens × 2 zoom, lower panels × 60 lens, × 3 zoom. (**d**) Co-localization of NLRP3 (magenta), ASC (red) and caspase-8 (green, FLICA) in untreated and treated HPTC (24 h) (×60 lens, × 3 zoom). All cells were background stained with DAPI (blue)

confirming ASC oligomerization during THF*α*/CHX-induced apoptosis in HPTC (Figures 6a and b). Using a similar approach in mouse TEC, active caspase-8 and ASC monomers emerged in the mitochondrial fraction following TNF*α*/CHX stimulation (Figure 6c). In contrast, caspase-8 activation and ASC expression at the mitochondria

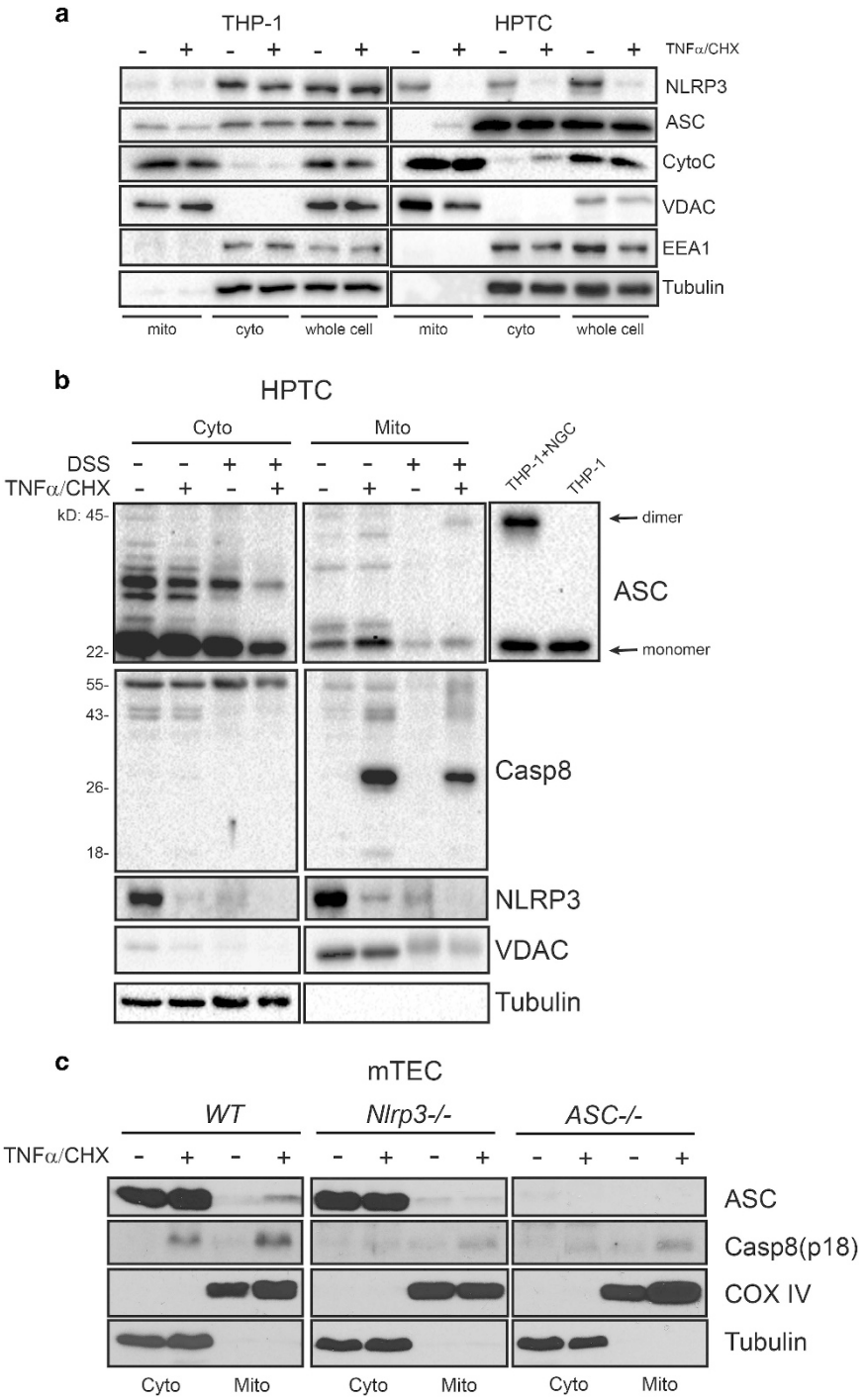

Figure 6 Cellular localization of NLRP3, ASC and Caspase-8. (**a**) Mitochondrial and cytoplasmic fractionation in HPTC and THP-1 macrophages at baseline and following TNFα (10 ng/ml)/CHX (25 μg/ml) treatment at 24 h. Immunoblotting for the indicated proteins. Cytochrome *c*/VDAC and tubulin/EEA1 are mitochondrial and cytoplasmic protein controls, respectively. (**b**) Cytosolic and mitochondrial fractionation of HPTC treated with TNF*α*/CHX at 24 h. Uncrosslinked and disuccinimidyl suberate (DSS)-crosslinked protein fractions were analyzed by immunoblotting as indicated. Arrows denote ASC monomer and dimer forms. Tubulin and the voltage-dependent anion channel, VDAC, are cytosolic and mitochondrial control markers, respectively. (**c**) Subcellular fractionations (cytosolic and mitochondrial) in wild-type (WT) *Nlrp3*−/− and *ASC*−/− TECs after 24 h treatment with TNFα (10 ng/ml)/CHX (5 μg/ml). Cytosolic fractions were chloroform/methanol precipitated before analysis for the indicated proteins (immunoblotting). Tubulin and COX IV are cytosolic and mitochondrial control markers, respectively

was reduced or absent in *Nlrp3−/−* and *ASC−/−* TECs. Together, these data support the immunofluorescence data and the conclusion that NLRP3, ASC and caspase-8 form a non-canonical protein complex at the mitochondria during receptor-mediated apoptosis in kidney epithelium.

NLRP3, ASC and caspase-8 complexes are activated by multiple mechanisms in epithelial cells. To assess the relationship between death receptor signaling and NLRP3-dependent apoptosis, experiments were performed examining RIP1, FADD and TRADD. As expected, the RIP1 inhibitor necrostatin-1 effectively blocked caspase-8 activation induced by TNF*α*/birinapant (Supplementary Figure S13a) but had no effect on caspase-8 activation or NLRP3/ASC/caspase-8 speck formation induced by TNF*α*/CHX (Supplementary Figures S13b and c). Next, siRNA was used to knock down TRADD and FADD in HPTC. Not surprisingly, in response to TNF*α*/CHX, both FADD and TRADD were required for optimal caspase-8 activation compared with control cells (Figure 7a). Using confocal microscopy, both FADD and TRADD colocalized to ASC specks, caspase-8 (FLICA) and NLRP3 in HPTC stimulated with TNF*α*/CHX (Figures 7b–d), supporting the involvement of TNFR signaling, FADD and TRADD in the activation of caspase-8 and the formation of NLRP3/ASC/caspase-8 complexes. The siRNA procedure, however, was not sufficient enough to detect a change in NLRP3/ASC/caspase-8 speck formation microscopically.

The NLRP3-dependent activation of caspase-8, however, may not be specific to any single apoptotic mechanism, and the co-localization of FADD/TRADD to NLRP3/ASC/caspase-8-positive specks may simply be a reflection of the involved death receptor pathway. In TECs treated with CHX alone, which can induce apoptosis through its effect on protein synthesis,[30,31] a small increase in cell death, apoptosis and caspase-8 activation could be observed that was dependent on Nlrp3 (Supplementary Figures S14a–c). Furthermore, induction of intrinsic apoptosis using etoposide also triggered caspase-8 and -9 activation in TECs that was dependent on Nlrp3 (Supplementary Figures S14d and e), suggesting that NLRP3 may represent a more generalized platform for caspase-8 activation at the mitochondria in epithelial cells.

Canonical inflammasome activation downstream of multiple pathogen and danger-associated molecular patterns is believed to converge on a single common pathway such as potassium (K+) efflux.[32] To examine the potential role of K+ efflux in the regulation of apoptosis and NLRP3/ASC/caspase-8 complex formation, HPTC were stimulated with TNF*α*/CHX in the presence of extracellular KCl and monitored for caspase-3 and -7 activity by live cell fluorescence microscopy. TNF*α*/CHX induced progressive apoptosis in HPTC that became detectable between 6 and 12 h and was effectively inhibited by extracellular KCl (Figure 8a). KCl also blocked TNF*α*/CHX-induced caspase-8 activation (Figure 8b). Consistent with these data, NLRP3/ASC/caspase-8 specks that are detectable as early as 12 h by fluorescence microscopy in TNF*α*/CHX-treated HPTC were absent and substantially reduced at 12 and 24 h, respectively, in the presence of extracellular KCl (Figure 8c). Thus these data show that NLRP3/ASC/caspase-8 complexes form in parallel with apoptosis in a process that is dependent on K+ efflux.

Nlrp3 regulates epithelial ASC speck formation in intestinal enteroids and during kidney injury *in vivo*. To confirm that ASC speck formation during apoptosis was not restricted to kidney epithelial cells, studies were performed in primary intestinal enteroids derived from the ceca of wild-type and *Nlrp3−/−* mice. Enteroids are comprised of an epithelial cell monolayer devoid of macrophages and other leukocytes.[33] Enteroids are also type II cells that cleave Bid in response to TNF*α*/CHX and undergo apoptosis, which disrupts the enteroid structure (Figures 9a and b). *Nlrp3−/−* enteroids displayed a significant reduction in caspase-8 activation and Bid cleavage following TNF*α*/CHX treatment compared with wild-type controls (Figures 9b and c). Similar to kidney epithelial cells, Nlrp3- and ASC-positive specks could be readily seen in TNF*α*/CHX-treated enteroids as cells became apoptotic and sloughed from the monolayer (Figure 9d). ASC speck formation was significantly reduced in *Nlrp3−/−* enteroids, confirming that Nlrp3 has a role in regulating this process during epithelial apoptosis (Figure 9d). These data support the concept that the regulation of caspase-8 by Nlrp3 during apoptosis may also occur in other epithelial tissues.

Our previous studies have demonstrated reduced epithelial cell apoptosis during tubular injury induced by UUO in *Nlrp3−/−* mice.[20] To determine whether epithelial cell injury in this model was associated with tubular ASC speck formation, wild-type, *Nlrp3−/−* and *ASC−/−* mice underwent UUO and the kidneys were analyzed by immunofluorescence microscopy. *Nlrp3−/−* kidneys displayed significantly less tubular staining for cleaved caspase-3 compared with wild-type kidneys following UUO injury at 14 days confirming a reduction in apoptosis (Figure 10a). In line with the *in vitro* studies, immunofluorescence revealed significant amounts of ASC-positive specks in E-cadherin-positive tubules in the injured wild-type kidneys that were substantially reduced or absent in *Nlrp3−/−*, *ASC−/−* or sham-treated mice (Figure 10b). Thus these data support the conclusion that Nlrp3 regulates epithelial cell apoptosis and tubular epithelial ASC speck formation during kidney injury *in vivo*.

Discussion

In this study, we elucidate the non-canonical function of NLRP3 in epithelium and highlight the ongoing crosstalk between the inflammasome and apoptosis machinery in the cell. NLRP3 and ASC form a non-canonical caspase-8-activating platform in epithelial cells that impacts apoptosis, a central process in the pathogenesis of kidney and gastrointestinal disease. The assembly of an NLRP3–ASC–caspase-8 protein complex described in this study occurred in the absence of caspase-1 or pro-inflammatory cytokine production and thus cannot be accurately described as an inflammasome. We propose that, in the absence of a clear inflammatory effector function, NLRP3 and ASC assembly at mitochondria in epithelial cells represents a non-canonical apoptosome for caspase-8 activation (Figure 10c).

The regulation of caspase-8 by NLRP3 identifies cell-context-specific functions for Nod-like receptors and inflammasomes in epithelial cells and leukocytes. The differential but related function of NLRP3 in these cell types also highlights the hierarchical organization of host defense

mechanisms that ensure appropriate responses to varying degrees of injury, essential to maintain tissue homeostasis. In macrophages and dendritic cells, the activation of caspase-8 occurs downstream of NLRP3, AIM2 and NLRC4 inflammasomes in response to canonical triggers such as dsDNA and *Salmonella* infection that contributes largely to

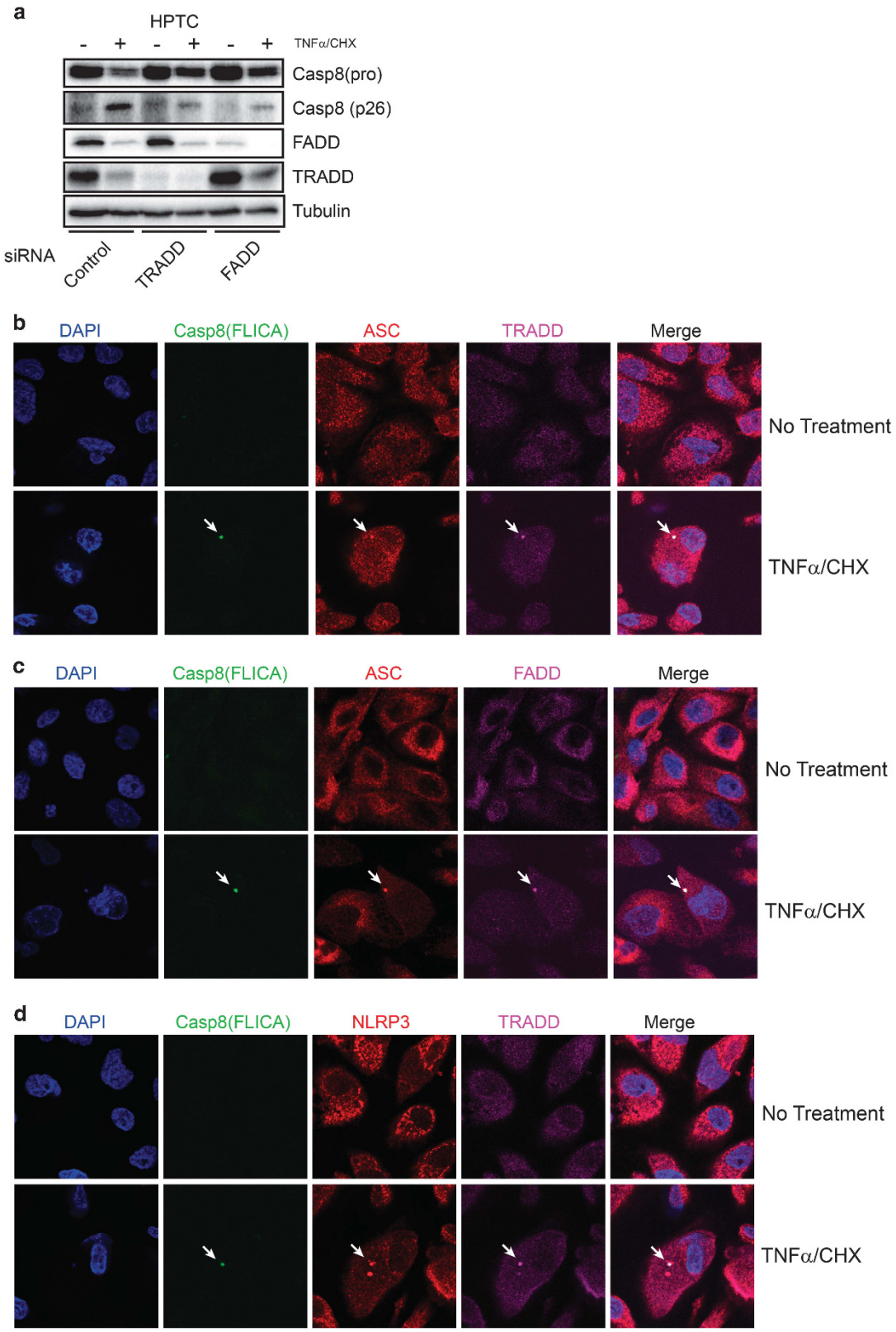

cytokine maturation.[4,12,13,16,17] Although inflammasome-dependent caspase-8 activation contributes to apoptosis in macrophages,[4,12] our data, in contrast, demonstrates a direct role for NLRP3 in receptor-mediated cell death independent of the inflammasome in epithelial cells. We do not detect NLRP3-dependent cytokine secretion or a canonical caspase-1-activating inflammasome in proximal tubular epithelial cells. The variables that determine inflammasome formation in kidney epithelial cells remain to be determined but not likely related to caspase-1 expression or cellular priming. The differential regulation of apoptosis and inflammasome activation between cell types, however, may be related to the cellular localization of NLRP3, which is largely cytoplasmic in macrophages and mitochondrial in tubular epithelial cells.

The effect of NLRP3 and ASC in the regulation of caspase-8 in tubular epithelial cells affected primarily the type II cell death phenotype where death receptor-mediated apoptosis requires mitochondrial amplification to fully execute apoptosis. Cardiolipin, which also interacts with NLRP3,[29] acts as an anchor and activating platform for caspase-8 in the mitochondria in type II apoptotic cells.[9] Several proteins have also been suggested to interact with caspase-8 in the mitochondria, including mitochondrial-antiviral signaling protein which is known to interact with NLRP3.[34–38] Whether any of these proteins or cardiolipin have a role in the assembly of an NLRP3-dependent-activating platform for caspase-8 remains to be determined.

The mechanism of NLRP3/ASC/caspase-8 complex formation does not appear to be specific to any single apoptosis pathway and may represent a general platform induced at the mitochondria regardless of the stimulus, similar to the mechanism of canonical NLRP3 inflammasome activation in macrophages. First, Nlrp3 regulated caspase-8 activation downstream of multiple pathways involving TNFR, CD95 and non-death receptor apoptosis triggered by etoposide. Second, the impact of K+ on epithelial cell apoptosis and the formation of the non-canonical NLRP3/ASC/caspase-8 platform implies that multiple mitochondrial cell death pathways may converge on a single mechanism to that involving NLRP3. Clearly more work is required to further dissect the essential players that regulate the NLRP3-dependent cell death pathway in epithelial cells.

In summary, our data provides insight into the role of NLRP3 in epithelial cells in response to injury. In addition to regulating the inflammasome and cytokine secretion in macrophages, NLRP3 regulates caspase-8 and apoptosis in the epithelium through the formation of a non-canonical protein complex at the mitochondria. This work emphasizes NLRP3 as a multifaceted protein that impacts, in a cell-context-specific manner, inflammation and death pathways that are central to tissue homeostasis, host response to infection/injury and the pathogenesis of disease.

Materials and Methods

Mice. *Nlrp3*$-/-$,[39] *ASC*$-/-$[40] and *caspase 1/11*$-/-$[41] were on a C57Bl/6 background and housed under standard conditions. Mice were used between 8 and 12 weeks of age. *Nlrp3*$-/-$ and wild-type C57Bl/6 control mice used in this study were derived from *Nlrp3*$-/+$ mice. Nlrp3 heterozygotes were derived from *Nlrp3*$-/-$ mice crossed with C57Bl/6 mice (Charles River, Wilmington, MA, USA). Unilateral ureteric obstruction model was performed as previously described.[20]

Primary cell culture. TECs were isolated from the kidneys harvested from mice between the ages of 8–12 weeks. Under sterile conditions, the capsules surrounding the kidneys were detached, and the renal cortex was removed with a sterile scalpel. Renal cortex tissues were placed in 1.5 mg/ml collagenase/HBSS (Sigma-Aldrich, St. Louis, MO, USA) solution and incubated at 37 °C with 5% CO_2 for 60 min. Tissue was homogenized using sterile microscope slides and then passed through 70-μm nylon filters. The cell suspension was spun down for 5 min at 230 × *g* to remove excess collagenase and washed twice more in 1 × HBSS. The cell pellet was resuspended in K1 media (10% fetal bovine serum (FBS), 1% penicillin–streptomycin, 1% hormone mix (ITSS media supplement, 350 nM prostagladin E_1, 5 nM 3,3′,5-triiodo-L-thyronine sodium salt, 5 μM hydrocortisone, 10 mM HEPES pH 7.4), 25 ng/ml mouse EGF, 25 mM HEPES pH 7.4 in DMEM/F12) and plated onto tissue culture plates for 1–2 h at 37 °C to remove contaminating fibroblasts and endothelial cells. The cell suspension was then re-plated onto collagen-IV-coated plates and allowed to grow overnight at 37 °C. Cells were washed and media changed the next day. Cells were maintained in K1 media and allowed to grow to confluence before passage onto experimental plates. All *in vitro* experiments were completed within two cell passages. Cells were confirmed to be epithelial cells periodically by ZO-1 or E-cadherin immunofluorescence staining for tight junction formation.

HPTCs were isolated from non-diseased nephrectomy samples from patients with renal cell carcinoma. Nephrectomy samples were placed in clean HBSS on ice for transport before isolation. Subsequent steps were performed in a biosafety cabinet under sterile conditions. The capsule and medulla were dissected away from the cortex. Minced renal cortex tissues were then placed in a 1.5 mg/ml collagenase/HBSS (Sigma) solution and incubated at 37 °C for 60 min. Tissue was homogenized using two sterile microscope slides and then passed through a 70-μm nylon filter. The filtered cell suspension was then spun down for 10 min at 230 × *g* to remove excess collagenase and washed two times in 1 × HBSS. The cell pellet was resuspended in HPTC media (10% FBS, 1% penicillin–streptomycin, 1% hormone mix, 25 ng/ml human EGF, 25 mM HEPES pH 7.4 in DMEM/F12) and plated onto uncoated tissue culture plates for 1 h at 37 °C. After 1 h, the cell suspension was re-plated onto collagen-IV-coated plates and allowed to grow overnight at 37 °C. Cells were washed and media changed the following day.

Bone marrow macrophages were isolated from the femurs and tibia of mice between the ages of 8–12 weeks. The bone marrow was collected on ice in HBSS. Cells were washed twice with HBSS and spun down at 230 × *g* for 5 min. Macrophages were plated onto tissue culture plates and maintained for 48 h in L929-cell media followed by a fresh media change. Macrophages were utilized 7 days after isolation.

Primary peritoneal macrophages were isolated from mice between the ages of 8–12 weeks. Mice were injected with 4% thioglycollate solution (BD Biosciences, San Jose, CA, USA) 72 h before peritoneal lavage. The peritoneal cavity was lavaged under sterile conditions with 10 ml RPMI media and kept on ice. The cells were spun down at 230 × *g* for 5 min before the addition of red cell lysis buffer for 5 min on ice. Cells were washed twice with RPMI media supplemented with 10% FBS, 1% penicillin–streptomycin and 50 nM 2-mercaptoethanol and plated onto tissue culture plates.

Mouse cecal enteroid cultures were established using protocols based on methods previously established by Sato *et al*.[33] Stem cell-containing intestinal crypts were recovered from the ceca of both wild-type C57BL/6 and *Nlrp3*$-/-$ mice. Briefly, the cecum was removed from male 8-week-old mice, cut open longitudinally and washed

Figure 7 Involvement of FADD and TRADD in caspase-8 activation and NLRP3/ASC speck formation. (**a**) Immunoblotting for pro-caspase-8, caspase-8 p26 cleavage product (N-terminal DED-domain) in HPTC transfected with control (scramble) siRNA or siRNAs targeting FADD and TRADD. HPTC were treated with TNFα (10 ng/ml)/CHX (25 μg/ml) and analyzed at 24 h. FADD and TRADD immunoblotting demonstrates efficacy of RNA interference and protein knock down. (**b**) Confocal immunofluorescence microscopy probing for activated caspase-8 (green, FLICA), ASC (red), TRADD (magenta) or (**c**) FADD (magenta) in HPTC treated with TNFα/CHX at 24 h. (**d**) Confocal immunofluorescence microscopy probing for activated caspase-8 (green, FLICA), NLRP3 (red) and TRADD (magenta) in HPTC treated with TNFα/CHX at 24 h (×60 lens, × 3 zoom). Arrows denote co-localizing proteins. Images are representative of two independent experiments

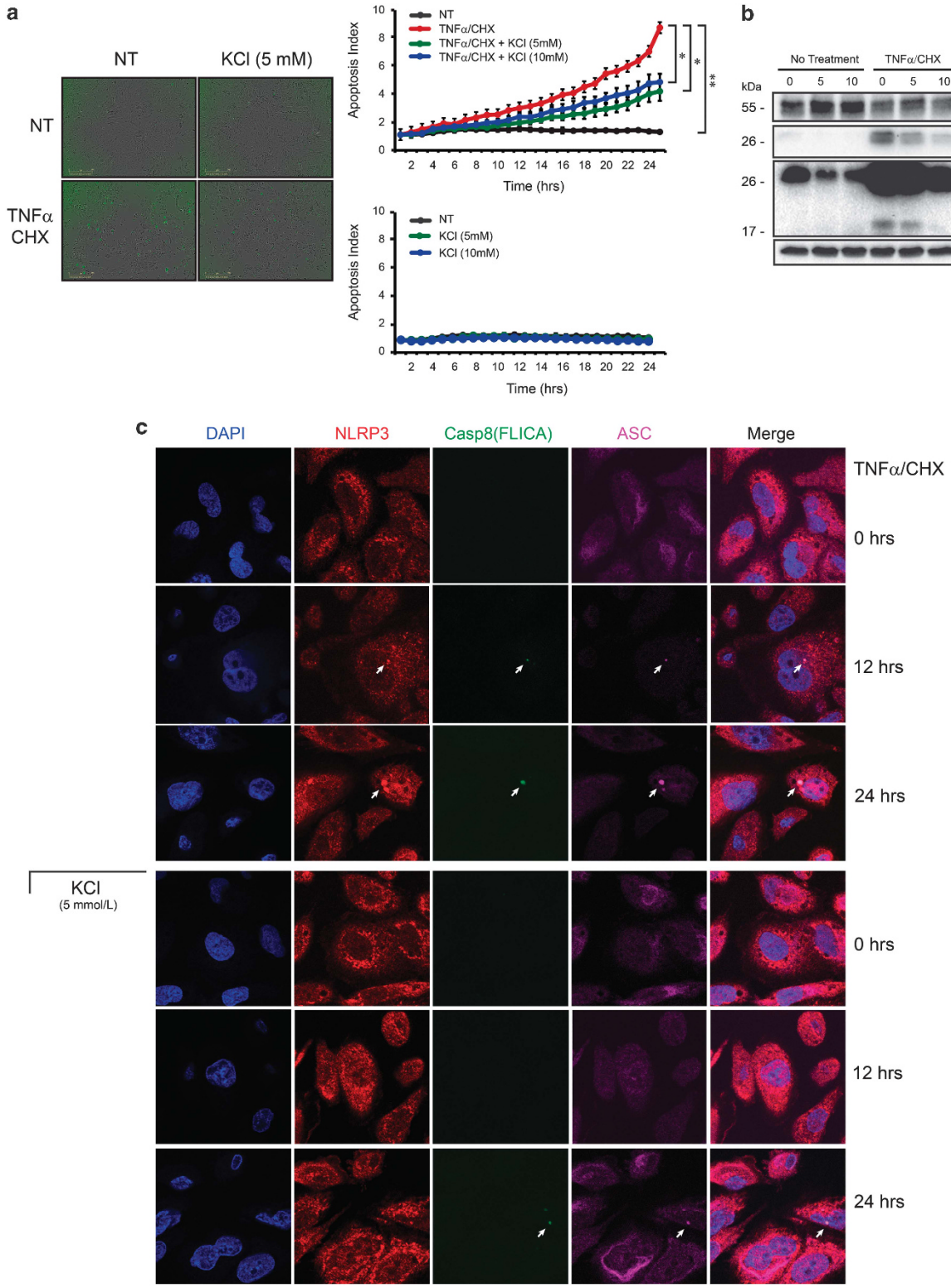

Figure 8 Potassium efflux and epithelial cell apoptosis, caspase-8 activation and NLRP3/ASC/caspase-8 complex formation. (**a**) Live cell fluorescence imaging and quantification of caspase-3 and -7 activity over a 24-h time course in HPTC untreated (NT) or TNFα (10 ng/ml)/CHX (25 μg/ml) stimulated with or without the addition of 5 or 10 mmol/l of extracellular KCl to the cell culture medium (mean $\pm$ S.E.M., $n=3$ for each time point. TNFα/CHX *versus* no treatment, $^{**}P<0.01$; TNFα/CHX *versus* TNFα/CHX+KCl, $^{*}P<0.05$). Left images of HPTC at 24 h treated with TNFα/CHX and extracellular KCL as indicated. Representative of experiment performed three times. (**b**) Immunoblotting for pro-caspase-8 and caspase-8 (p26 and p18) in TNFα/CHX-treated HTPC cultured in 0, 5 or 10 mmol/l of extracellular KCl at 24 h. (**c**) Confocal immunofluorescence microscopy probing for activated caspase-8 (green, FLICA), NLRP3 (red) and ASC (magenta) in HPTC treated with TNFα/CHX at 0, 12 and 24 h with or without the addition of 5 mmol/l of extracellular potassium to the cell culture medium (×60 lens, ×3 zoom). Arrows denote NLRP3/ASC/caspase-8-positive specks. Representative images of two independent experiments

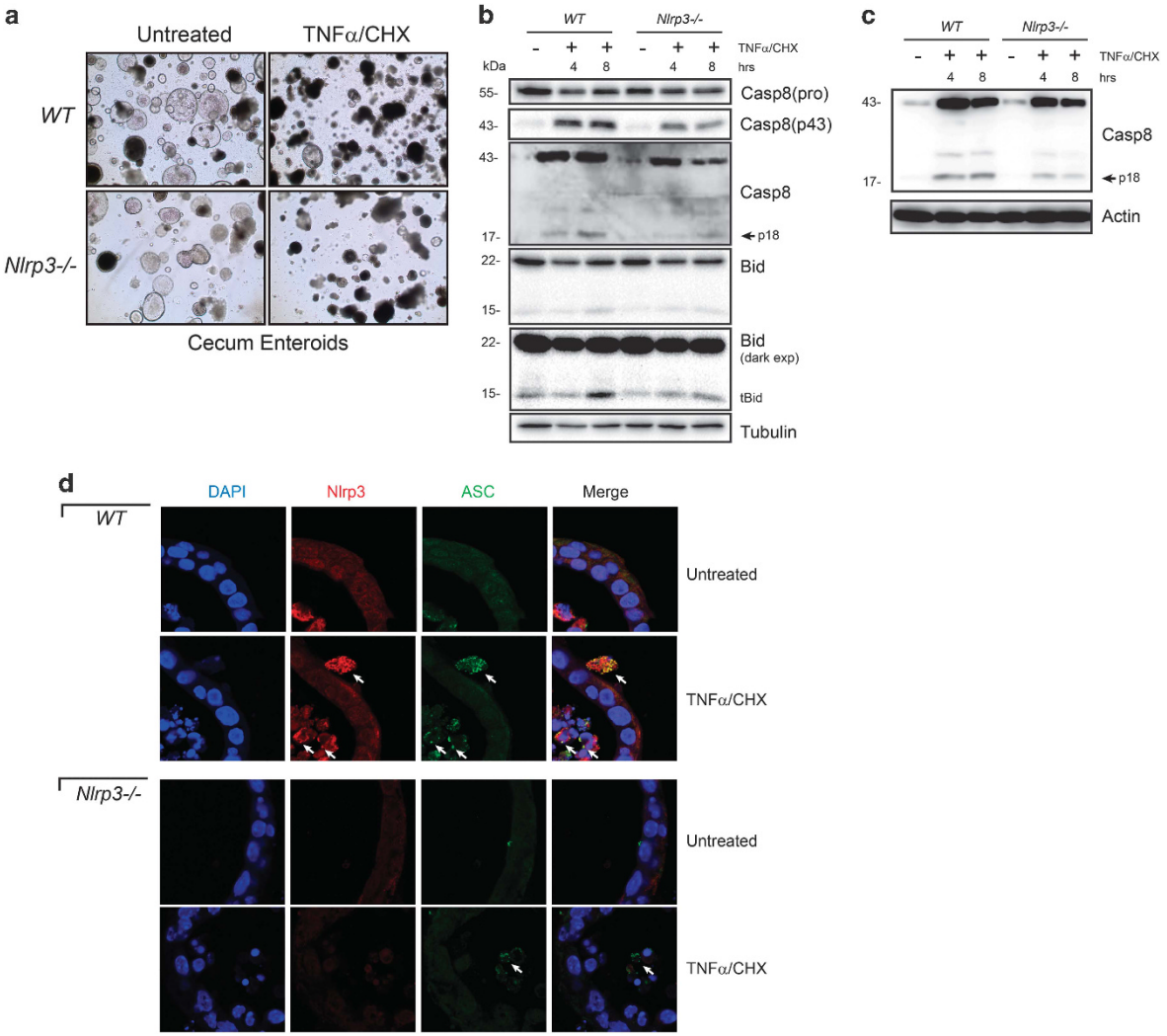

Figure 9 Nlrp3-dependent caspase-8 activation and ASC speck formation in cecal-derived enteroids. (**a**) Brightfield microscopy of cecal enteroids suspended in matrigel following 7 days of growth at ×4 magnification. Healthy wild-type (WT) and *Nlrp3*−/− enteroids (left panels) are compared against enteroids following 6 h of exposure to TNFα (10 ng/ml)/CHX (5 μg/ml) (right panels). (**b**) Immunoblotting for caspase-8 (pro, p43 and p18) and Bid in WT and *Nlrp3*−/− cecal enteroids treated with TNFα/CHX. (**c**) Immunoblotting for caspase-8 in a second independent set of WT and *Nlrp3*−/− cecal enteroids at 4 and 8 h following exposure to TNFα/CHX. (**d**) Immunofluorescence confocal microscopy of untreated and TNFα/CHX treated WT and *Nlrp3*−/− cecal enteroids. NLRP3 (red), ASC (green) and DAPI (blue) at ×100 magnification. Co-localized NLRP3 and ASC specks are visible in WT cells at various stages of apoptosis and sloughing but not in *Nlrp3*−/− cells and only rarely in WT healthy cells still maintaining the enteroid's epithelial monolayer

repeatedly in sterile PBS containing gentamicin and penicillin/streptomycin. The washed cecal tissue was incubated for 30 min at 4 °C in cell recovery solution (Corning, NY, USA) to detach the cecal epithelium from the surrounding muscle and connective tissue. The epithelium was gently scraped off and then vortexed briefly to detach individual crypts. Crypts were washed twice in Advanced DMEM/F12 containing penicillin/streptomycin, HEPES buffer and Glutamax (Gibco, Thermo-Fisher Scientific, Waltham, MA, USA, hereby referred to as MEM+++), suspended in matrigel (Corning), and plated as 30–40 μl drops in 24-well plates (Corning). Cecal enteroids were grown routinely in growth media containing MEM+++, R-spondin, Noggin and Wnt3A conditioned media,[42] N2 supplement (Invitrogen, Grand Island, NY, USA), B27 supplement (Invitrogen), mEGF (Invitrogen), A83-01 (Tocris, Bristol, UK), SB202190 (Sigma-Aldrich), *N*-acetylcysteine (Sigma-Aldrich) and nicotinamide (Sigma-Aldrich), as described by Sato *et al*.[33] The media was changed every 2–3 days, and the resultant enteroid cultures were split one to four, every 7 days.

This growth medium allowed for the rapid growth and propagation of mouse cecal enteroids, however, the addition of Wnt3A, A83-01, SB202190 and nicotinamide is known to inhibit the differentiation and maturation of certain cell types, including mature enterocytes and goblet cells.[33] To account for this in experimental cultures, 4 days prior to treatment with TNFα/CHX, nicotinamide, A83-01 and SB202190 were omitted from the media, and the Wnt3A conditioned media was reduced by 50%, with the volume being balanced with additional MEM+++. Twenty four hours prior to treatment, the Wnt3A conditioned medium was omitted entirely as well and 100 ng/ml LPS (Sigma-Aldrich) was supplemented.

The human myelogenous leukemia THP-1 cell line were purchased from the American Type Culture Collection (ATCC, Manassas, VA, USA). THP-1 cells were cultured in RPMI 1640 media (Gibco, Thermo-Fisher Scientific) supplemented with 10% v/v heat-inactivated FBS, 0.05 mM β-mercaptoethanol and 1 mM sodium pyruvate. Cells were maintained in cell suspension in a 37 °C, 5% CO_2, humidified incubator. Cells were differentiated with 100 nM phorbol-12-myristate-13-acetate (Sigma-Aldrich) for 24 h prior to experiments.

Apoptosis and inflammasome activation. Tubular epithelial cells and macrophages were counted before final plating onto experimental plates. Twelve-well plates were seeded with 25 000 cells/well. Six-well plates were seeded with 100 000 cells/well. For apoptosis experiments, cells were serum starved overnight

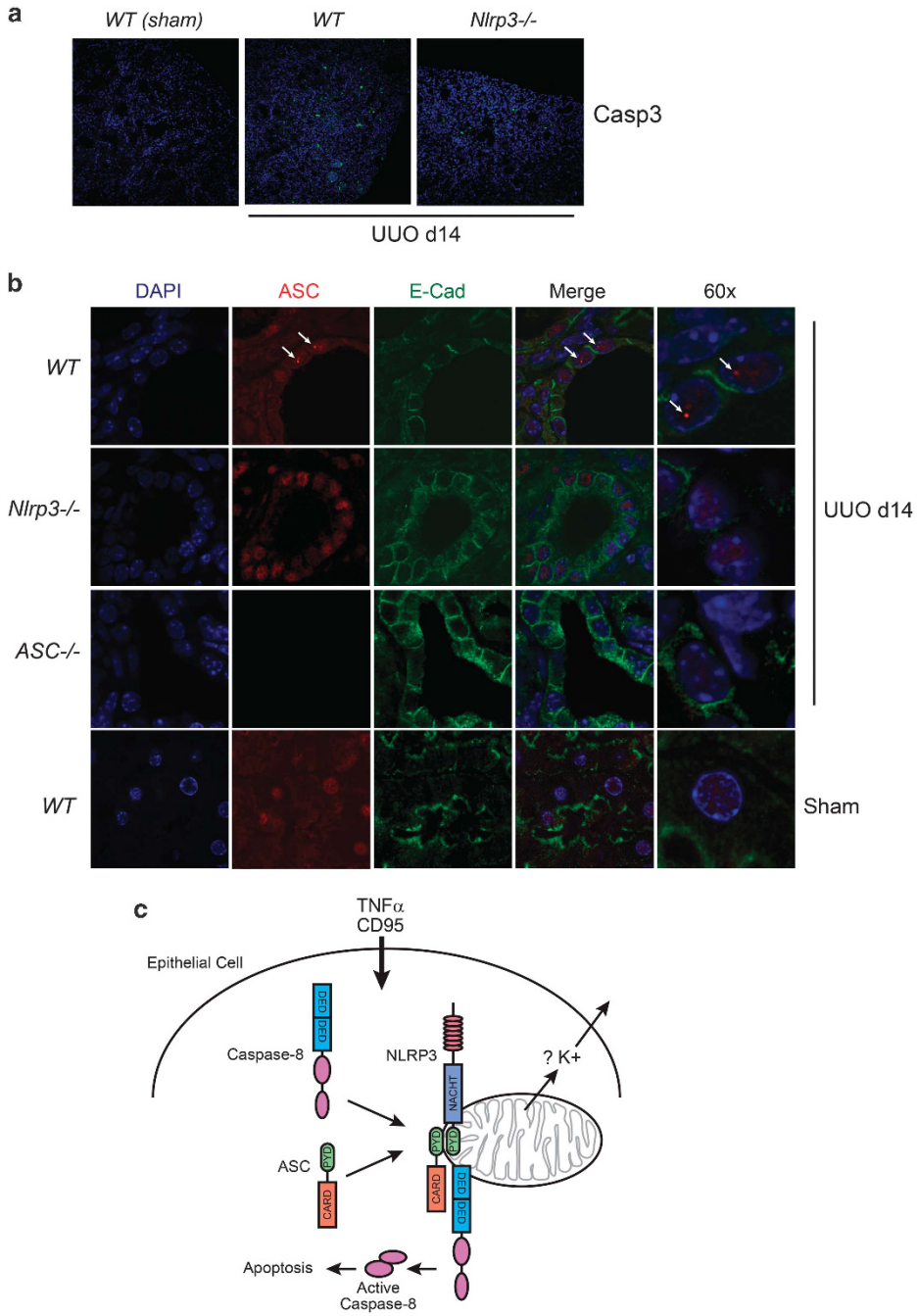

Figure 10 Apoptosis and ASC speck formation in kidney tubular epithelium *in vivo*. (**a**) Immunofluorescence probing for activated (cleaved) caspase-3 in the wild-type (WT) or *Nlrp3*−/− kidney 14 days following UUO (×20 lens). (**b**) Immunofluorescence for ASC and E-cadherin in the WT, *Nlrp3*−/− and *ASC*−/− kidneys at 14 days following UUO. Sham-operated WT mice are shown as controls (×60 lens, ×4 zoom, far right panels ×10 zoom). Arrows denote ASC speck formation in E-cadherin-positive tubular epithelial cells. (**c**) Proposed model of NLRP3-dependent caspase-8 activation during epithelial cell apoptosis

and treated with the following reagents: TNFα (10 ng/ml), CHX (5 μg/ml for mouse TEC, enteroids and 25 μg/ml for HPTC, Sigma-Aldrich), birinapant 10 μM (Apexbio, Houston, TX, USA), necrostatin-1 (10 μM, Sigma-Aldrich), etoposide (100–1000 μM, Sigma-Aldrich), and hamster anti-mouse CD95/Fas antibody 40 μg/ml (Jo2 clone, BD Biosciences), were added at the initiation of the experiment and allowed to incubate for the indicated time points at 37 °C. For inflammasome activation experiments, epithelial cells and macrophages were primed with 100 ng/ml ultrapure LPS as above before incubation for 6 or 24 h with 250 μg/ml MSU, 5 mM ATP or 20 μM nigericin. Supernatants and cell protein lysates were harvested for analysis.

IL-1β and IL-18 ELISAs. TECs were primed overnight with 100 ng/ml ultrapure LPS before incubation for 24 h with TNFα (10 ng/ml)+CHX (5 μg/ml), MSU 25 μg/ml or ATP (5 mM). Bone marrow macrophages were incubated with 5 mM ATP for 6 h as a positive control. IL-1β and IL-18 cytokine secretion was detected in cell supernatants using the ELISA kits from BD Biosciences and eBiosciences (San Diego, CA, USA), respectively, as per the manufacturers' protocol.

Immunoblotting. Protein samples were separated on SDS-PAGE gels under reducing conditions. Proteins were transferred onto nitrocellulose membranes, which were blocked for 1 h with the appropriate blocking solution before incubating

overnight at 4 °C with the primary antibody. Blots were washed with an appropriate buffer and then incubated at room temperature with the secondary antibody in blocking buffer for 1 h before additional washes. Proteins were visualized using ECL western blotting detection reagents (GE Healthcare, Pittsburgh, PA, USA) and exposed to film or digitally captured using a Chemidoc MP device (Bio-Rad, Hercules, CA, USA). Bands were quantified using the ImageJ (NIH, Bethesda, MD, USA) or Image Lab (Bio-Rad) software and normalized as indicated. Antibodies used are as follows: mouse anti-human NLRP3 (Cryo-2 clone, Adipogen), rabbit anti-human ASC (Adipogen, San Diego, CA, USA), rabbit anti-human PARP1 and cleaved PARP1 (Cell Signaling, Danvers, MA, USA nos. 9542 and 9544), rabbit anti-human caspase-3 (Cell Signaling no. 9662), rabbit anti-mouse caspase-8 (Cell Signaling nos. 8592, 9429 and 4927), rabbit anti-mouse Bid (Abcam, Cambridge, UK no. 10640), rat anti-mouse Bid (clone 8C3, generous gift from Dr. Thomas Kaufmann, University of Bern, Bern, Switzerland), mouse anti-human caspase-9 (Cell Signaling no. 9508), rabbit anti-mouse caspase-1 (Santa Cruz, Dallas, TX, USA, no. 514), rat anti-mouse caspase-11 (Novus Biologicals, Littleton, CO, USA), rabbit anti-human FLIP (Santa Cruz no. 8346), mouse anti-cow COX IV (Abcam no. 14744), rabbit anti-human EEA1 (Abcam no. 2900), rabbit anti-human cytochrome *c* (Abcam no. 133504), rabbit anti-human XIAP (Cell Signaling no. 2042), rabbit anti-human caspase-8 (Cell Signaling no. 9496), mouse anti-human caspase-8 (Cell Signaling no. 9746), rabbit anti-human VDAC (Cell Signaling no. 4866), rabbit anti-human caspase-1 (Santa Cruz, no. 622 antibody against N-terminal CARD domain), mouse anti-human FADD (Santa Cruz no. 271748), rabbit anti-human TRADD (Santa Cruz no. 7868), rabbit anti-human RIP-1 (Cell Signaling no. 3493), rabbit anti-human TRAF2 (Santa Cruz no. 877), mouse anti-human β-tubulin (clone D66, Sigma-Aldrich), and rabbit anti-mouse β-actin (Cell Signaling).

Annexin V labeling, MTT assay and incucyte zoom microscopy. Wild-type and *Nlrp3*$-/-$ TECs were grown to monolayer before treatment with CHX and TNFα. Annexin V–FITC (BD Biosciences) and Sytox orange (Molecular Probes, Thermo Fisher Scientific, Waltham, MA, USA) was used to label apoptotic and necrotic TECs, respectively, and imaged over 24 h by fluorescent wide field microscope (Olympus, Center Valley, PA, USA). Annexin V and Sytox orange positivity was quantified by ImageJ analysis.

TECs were assessed for cell viability using the MTT assay (Invitrogen) as per the manufacturer's instructions. Tubular epithelial cells were grown to monolayer and treated with various reagents for 24 h in serum-free media. Cells were incubated with MTT reagent (12 mM) for 4 h at 37 °C. Viable cells converted MTT to insoluble formazan crystals, which was solubilized by DMSO before quantification by spectrophotometer (Molecular Devices, Sunnyvale, CA, USA) at 540 nM. Cell viability was calculated for each treatment relative to untreated cells.

Tubular epithelial cells were grown to monolayer and induced to undergo apoptosis in serum-free media with or without incubation in 5 or 10 mM of KCl. Cells were treated with CellPlayer Kinetic Caspase 3/7 Reagent (Essen Bioscience, Ann Arbor, MI, USA) to label apoptotic cells. Images were taken using an automated fluorescent microscope (Incucyte Zoom, Essen Bioscience) over a 24-h time course at 37 °C. Apoptosis index was calculated by quantifying the number of apoptotic cells relative to the total number of cells per field and normalized as a fold change relative to time zero within each treatment.

Subcellular fractionations. HPTC subcellular fractionations were performed on untreated cells or treated with TNFα/CHX. Cells were collected in 1 ml of mannitol buffer (10 mM HEPES, 70 mM Sucrose, 210 mM D-Mannitol, 0.1 mM EGTA, pH 7.4) containing protease inhibitor cocktail (Roche, Mississauga, ON, Canada). Fifteen strokes through a 27-G needle were performed to homogenize the cells, and the homogenate was spun at $320 \times g$ for 5 min to remove unbroken cells. The soluble fraction was spun at $8000 \times g$ for 15 min to collect crude mitochondrial fraction. The pellet containing mitochondria was washed in 1 ml of PBS twice and re-suspended in 0.5 M sucrose and gently layered on discontinuous sucrose gradient (30% w/w. 40% w/w, 50% w/w, 60% w/w) containing 1 mM EDTA, 0.1% BSA, 10 mM Tris-HCl (pH 7.5). After ultracentrifugation at $51\,000 \times g$ for 3 h at 4 °C, intact mitochondrial band was collected and pelleted by additional centrifugation at $26\,000 \times g$ for 30 min at 4 °C. To preserve oligomer form of ASC, 2 mM of disuccinimidyl suberate was used to crosslink proteins. Mouse TEC subcellular fractionations were completed at 4 °C using the mitochondrial isolation kit for cultured cells from Thermo Fisher Scientific. Fractionations were carried out using the manufacturer's instructions.

Mitochondrial fractions were resuspended in 3× SDS sample buffer containing 0.1% Triton-X100 in preparation for immunoblotting. Samples were boiled for 5 min before loading into denaturing SDS gels for analysis. Cytosolic fractions were precipitated using chloroform and methanol and resuspended in an equivalent amount of sample buffer as the mitochondrial pellet. Briefly, four volumes of methanol were added to the cytosolic fraction and vortexed before the addition of one volume of chloroform. Samples were vortexed once again and three volumes of H_2O were added followed by additional vortexing. Samples were spun at $15\,000 \times g$ for 2 min, and the aqueous layer was removed. Four volumes of methanol were finally added, and the samples were vortexed and spun for a final time at $15\,000 \times g$ for 2 min. The remaining liquid was completely removed, and the resulting precipitate was resuspended in sample buffer. Fractions were characterized using immunoblotting and antibodies against tubulin, EEA1 (cytosolic), VDAC and COX IV (mitochondrial).

RNA interference. HPTC were trypsinized and one million cells were nucleofected with 30 pmol of non-targeting (5′-UAGCGACUAAACACAUCAA-3′) or SMARTpool small interfering RNAs of *FADD* (with the following sequences: 5′-CAGCAUUUAACGUCAUAUG-3′; 5′-UGCAGCAUUUAACGUCAUA-3′; 5′-GUGCAGCAUUUAACGUCAU-3′; 5′-GAACUCAAGCUGCGUUUAU-3′) or *TRADD* (with the following sequences: 5′-GGAGGAUGCGCUGCGAAAU-3′; 5′-GCGAGGGACUGUACGAGCA-3′; 5′-GGGUCAGCCUGUAGUGAAU-3′; 5′-GGACGAGGAGCGCUGUUUG-3′) (Dharmacon, Lafayette, CO, USA) using the Nucleofection Technology (Amaxa, London, UK) according to the manufacturer's protocols. Transfected cells were seeded in a six-well plate (0.5×10^6/well) and incubated for 48 h before treatment. Efficacy of gene knockdown was confirmed by immunoblotting.

Immunofluorescence microscopy. HPTCs were grown to 70% confluency on sterile collagen-coated coverslips. Cells were stimulated with TNFα (10 ng/ml) and CHX (25 μg/ml) or mock treated in serum-free media for 24 h prior to fixation, and cells were incubated with 300 μl 1× FAM-LETD-fmk (FLICA-caspase-8, Immunochemistry Inc., Bloomington, MN, USA) or FAM-YVAD-fmk (FLICA-caspase-1) or Mitotracker red (100 nM, Molecular Probes, Thermo-Fisher Scientific) for 1 h. FLICA-treated cells were washed in wash buffer according to the manufacturer's protocol. Cells were then washed in PBS and fixed in 4% paraformaldehyde followed by incubation with NH_4Cl (50 μM) for 10 min to reduce auto-fluorescence and permeabilization with 0.1% Triton X-100 for 5 min. Cells were blocked in 3% BSA for 30 min at room temperature and then incubated with primary antibodies (1:100) in blocking solution for 1 h at room temperature. Antibodies used in the experiments are mouse anti-human NLRP3 (Cryo-2, Adipogen), rabbit anti-human ASC (Adipogen), mouse anti-human E-Cadherin (BD Biosciences no. 610181), rabbit anti-human LAMP1 (Abcam no. 24170), mouse anti-human FADD (Santa Cruz), rabbit anti-human TRADD (Santa Cruz) and rabbit anti-human GM130 (Abcam no. 52649). Following sequential washes in PBS, cells were incubated with secondary fluorescent antibodies (1:600, Alexa Fluor, Thermo-Fisher Scientific) in blocking solution for 1 h at room temperature. Coverslips were mounted onto slides in ProlongGold antifade reagent containing 4′,6-diamidino-2-phenylindole (DAPI, Molecular Probes, Thermo-Fisher Scientific). For *in vivo* studies, immunofluorescence microscopy was performed on the kidneys from mice 14 days after UUO. Kidneys were removed and prepared for immunoblotting or histology using 10% formalin fixation. Paraffin-embedded kidney tissue sections were deparaffinized, blocked and stained with E-Cadherin (BD Biosciences), ASC (Adipogen) and cleaved caspase-3 antibodies (Cell Signaling) using standard staining protocols. Confocal microscopy was performed on an Olympus IX-70 microscope with the Fluoview1000 system software (Center Valley, PA, USA).

Enteroid cultures used for immunofluorescent microscopy were fixed overnight with 10% formalin, 1 h posttreatment with TNFα/CHX. Following formalin fixation, enteroids were washed in PBS, resuspended in 3% low-melting point agarose, embedded in paraffin and sectioned onto microscope slides. Sections were deparaffinized with xylene and rehydrated in 100, 95 and 75% ethanol, followed by deionized water. Antigen retrieval was performed by boiling in sodium citrate buffer for 30 min. Sections were blocked with goat serum for 1 h at RT and treated with anti-NLRP3 and anti-ASC primary antibodies (1:100) in blocking buffer overnight at 4 °C. Following two PBS washes, sections were incubated with appropriate secondary antibodies (1:1000, Thermo-Fisher Scientific) for 1 h at RT and washed twice in PBS and once in H_2O. Coverslips were mounted onto slides in ProlongGold antifade reagent containing DAPI (Molecular Probes, Thermo-Fisher Scientific), and confocal microscopy was performed with a Leica SP5 Microscope with the Leica application suite software (Buffalo Grove, IL, USA).

Statistical analysis and ethics. All studies using mice or human tissues were approved by the Animal Care Committee and the Conjoint Health Research

Ethics Board at the University of Calgary, respectively. Except where indicated, all experiments were performed at least three independent times. GraphPad Instat software (La Jolla, CA, USA) was used to perform all statistical analyses. Data were expressed as mean $\pm$ S.D. or S.E.M. as indicated. Results were analyzed for statistical variance using an unpaired Student's *t*-test or ANOVA where appropriate. Results at $P < 0.05$ were considered statistically significant.

Conflict of Interest

The authors declare no conflict of interest.

Acknowledgements. This work was supported by operating grants from the Canadian Institutes for Health Research (to BAV and DAM), the Kidney Foundation of Canada (to DAM) and the Crohn's and Colitis Canada (CCC) (to BAV). Research was also supported by the Canadian National Transplantation Research Program (CNTRP) and the CIHR Inflammation in Chronic Disease Signature Initiative (to DAM). We thank Sharon A Clark for her technical support as well as the infrastructure and technical support provided by the Live Cell Imaging Facility at the Snyder Institute for Chronic Diseases. DAM holds a Tier II Canada Research Chair and a Clinical Senior Scholar award from Alberta Innovates Health Solutions (AIHS). BAV holds the Children with Intestinal and Liver Disorders (CH.I.L.D.) Foundation Research Chair in Pediatric Gastroenterology. PLB holds a Clinical Senior Scholar award from AIHS. JMP and AL are supported by Beverley Phillips Trainee Awards from the Snyder Institute for Chronic Disease, University of Calgary. MS is supported by a fellowship from the Michael Smith Foundation for Health Research (MSFHR), while VM is supported by a joint fellowship from the MSFHR and CCC.

1. Sutterwala FS, Haasken S, Cassel SL. Mechanism of NLRP3 inflammasome activation. *Ann NY Acad Sci* 2014; **1319**: 82–95.
2. Anders HJ, Muruve DA. The inflammasomes in kidney disease. *J Am Soc Nephrol* 2011; **22**: 1007–1018.
3. Knodler LA, Crowley SM, Sham HP, Yang H, Wrande M, Ma C *et al.* Noncanonical inflammasome activation of caspase-4/caspase-11 mediates epithelial defenses against enteric bacterial pathogens. *Cell Host Microbe* 2014; **16**: 249–256.
4. Sagulenko V, Thygesen SJ, Sester DP, Idris A, Cridland JA, Vajjhala PR *et al.* AIM2 and NLRP3 inflammasomes activate both apoptotic and pyroptotic death pathways via ASC. *Cell Death Differ* 2013; **20**: 1149–1160.
5. Kayagaki N, Warming S, Lamkanfi M, Vande Walle L, Louie S, Dong J *et al.* Non-canonical inflammasome activation targets caspase-11. *Nature* 2011; **479**: 117–121.
6. Kantari C, Walczak H. Caspase-8 and bid: caught in the act between death receptors and mitochondria. *Biochim Biophys Acta* 2011; **1813**: 558–563.
7. Jost PJ, Grabow S, Gray D, McKenzie MD, Nachbur U, Huang DC *et al.* XIAP discriminates between type I and type II FAS-induced apoptosis. *Nature* 2009; **460**: 1035–1039.
8. Scaffidi C, Schmitz I, Zha J, Korsmeyer SJ, Krammer PH, Peter ME. Differential modulation of apoptosis sensitivity in CD95 type I and type II cells. *J Biol Chem* 1999; **274**: 22532–22538.
9. Gonzalvez F, Schug ZT, Houtkooper RH, MacKenzie ED, Brooks DG, Wanders RJ *et al.* Cardiolipin provides an essential activating platform for caspase-8 on mitochondria. *J Cell Biol* 2008; **183**: 681–696.
10. Li H, Zhu H, Xu CJ, Yuan J. Cleavage of BID by caspase 8 mediates the mitochondrial damage in the Fas pathway of apoptosis. *Cell* 1998; **94**: 491–501.
11. Du C, Fang M, Li Y, Li L, Wang X. Smac, a mitochondrial protein that promotes cytochrome c-dependent caspase activation by eliminating IAP inhibition. *Cell* 2000; **102**: 33–42.
12. Pierini R, Juruj C, Perret M, Jones CL, Mangeot P, Weiss DS *et al.* AIM2/ASC triggers caspase-8-dependent apoptosis in Francisella-infected caspase-1-deficient macrophages. *Cell Death Differ* 2012; **19**: 1709–1721.
13. Man SM, Hopkins LJ, Nugent E, Cox S, Gluck IM, Tourlomousis P *et al.* Inflammasome activation causes dual recruitment of NLRC4 and NLRP3 to the same macromolecular complex. *Proc Natl Acad Sci USA* 2014; **111**: 7403–7408.
14. Man SM, Tourlomousis P, Hopkins L, Monie TP, Fitzgerald KA, Bryant CE. Salmonella infection induces recruitment of Caspase-8 to the inflammasome to modulate IL-1beta production. *J Immunol* 2013; **191**: 5239–5246.
15. Karki R, Man SM, Malireddi RK, Gurung P, Vogel P, Lamkanfi M *et al.* Concerted activation of the AIM2 and NLRP3 inflammasomes orchestrates host protection against aspergillus infection. *Cell Host Microbe* 2015; **17**: 357–368.
16. Ganesan S, Rathinam VA, Bossaller L, Army K, Kaiser WJ, Mocarski ES *et al.* Caspase-8 modulates dectin-1 and complement receptor 3-driven IL-1beta production in response to beta-glucans and the fungal pathogen, *Candida albicans*. *J Immunol* 2014; **193**: 2519–2530.
17. Gringhuis SI, Kaptein TM, Wevers BA, Theelen B, van der Vlist M, Boekhout T *et al.* Dectin-1 is an extracellular pathogen sensor for the induction and processing of IL-1beta via a noncanonical caspase-8 inflammasome. *Nat Immunol* 2012; **13**: 246–254.
18. Grgic I, Campanholle G, Bijol V, Wang C, Sabbisetti VS, Ichimura T *et al.* Targeted proximal tubule injury triggers interstitial fibrosis and glomerulosclerosis. *Kidney Int* 2012; **82**: 172–183.
19. Hirota SA, Ng J, Lueng A, Khajah M, Parhar K, Li Y *et al.* NLRP3 inflammasome plays a key role in the regulation of intestinal homeostasis. *Inflamm Bowel Dis* 2011; **17**: 1359–1372.
20. Vilaysane A, Chun J, Seamone ME, Wang W, Chin R, Hirota S *et al.* The NLRP3 inflammasome promotes renal inflammation and contributes to CKD. *J Am Soc Nephrol* 2010; **21**: 1732–1744.
21. Wang W, Wang X, Chun J, Vilaysane A, Clark S, French G *et al.* Inflammasome-independent NLRP3 augments TGF-beta signaling in kidney epithelium. *J Immunol* 2013; **190**: 1239–1249.
22. Bakker PJ, Butter LM, Claessen N, Teske GJ, Sutterwala FS, Florquin S *et al.* A tissue-specific role for Nlrp3 in tubular epithelial repair after renal ischemia/reperfusion. *Am J Pathol* 2014; **184**: 2013–2022.
23. Shigeoka AA, Mueller JL, Kambo A, Mathison JC, King AJ, Hall WF *et al.* An inflammasome-independent role for epithelial-expressed Nlrp3 in renal ischemia-reperfusion injury. *J Immunol* 2010; **185**: 6277–6285.
24. Wang L, Du F, Wang X. TNF-alpha induces two distinct caspase-8 activation pathways. *Cell* 2008; **133**: 693–703.
25. Benetatos CA, Mitsuuchi Y, Burns JM, Neiman EM, Condon SM, Yu G *et al.* Birinapant (TL32711), a bivalent SMAC mimetic, targets TRAF2-associated cIAPs, abrogates TNF-induced NF-kappaB activation, and is active in patient-derived xenograft models. *Mol Cancer Ther* 2014; **13**: 867–879.
26. Bossaller L, Chiang PI, Schmidt-Lauber C, Ganesan S, Kaiser WJ, Rathinam VA *et al.* Cutting edge: FAS (CD95) mediates noncanonical IL-1beta and IL-18 maturation via caspase-8 in an RIP3-independent manner. *J Immunol* 2012; **189**: 5508–5512.
27. Bracey NA, Gershkovich B, Chun J, Vilaysane A, Meijndert HC, Wright JR Jr. *et al.* Mitochondrial NLRP3 protein induces reactive oxygen species to promote Smad protein signaling and fibrosis independent from the inflammasome. *J Biol Chem* 2014; **289**: 19571–19584.
28. Zhou R, Yazdi AS, Menu P, Tschopp J. A role for mitochondria in NLRP3 inflammasome activation. *Nature* 2011; **469**: 221–225.
29. Iyer SS, He Q, Janczy JR, Elliott EI, Zhong Z, Olivier AK *et al.* Mitochondrial cardiolipin is required for Nlrp3 inflammasome activation. *Immunity* 2013; **39**: 311–323.
30. Martin SJ, Lennon SV, Bonham AM, Cotter TG. Induction of apoptosis (programmed cell death) in human leukemic HL-60 cells by inhibition of RNA or protein synthesis. *J Immunol* 1990; **145**: 1859–1867.
31. Tang D, Lahti JM, Grenet J, Kidd VJ. Cycloheximide-induced T-cell death is mediated by a Fas-associated death domain-dependent mechanism. *J Biol Chem* 1999; **274**: 7245–7252.
32. Petrilli V, Papin S, Dostert C, Mayor A, Martinon F, Tschopp J. Activation of the NALP3 inflammasome is triggered by low intracellular potassium concentration. *Cell Death Differ* 2007; **14**: 1583–1589.
33. Sato T, Vries RG, Snippert HJ, van de Wetering M, Barker N, Stange DE *et al.* Single Lgr5 stem cells build crypt-villus structures in vitro without a mesenchymal niche. *Nature* 2009; **459**: 262–265.
34. Milovic-Holm K, Krieghoff E, Jensen K, Will H, Hofmann TG. FLASH links the CD95 signaling pathway to the cell nucleus and nuclear bodies. *EMBO J* 2007; **26**: 391–401.
35. Stegh AH, Barnhart BC, Volkland J, Algeciras-Schimnich A, Ke N, Reed JC *et al.* Inactivation of caspase-8 on mitochondria of Bcl-xL-expressing MCF7-Fas cells: role for the bifunctional apoptosis regulator protein. *J Biol Chem* 2002; **277**: 4351–4360.
36. El Maadidi S, Faletti L, Berg B, Wenzl C, Wieland K, Chen ZJ *et al.* A novel mitochondrial MAVS/Caspase-8 platform links RNA virus-induced innate antiviral signaling to Bax/Bak-independent apoptosis. *J Immunol* 2014; **192**: 1171–1183.
37. Park S, Juliana C, Hong S, Datta P, Hwang I, Fernandes-Alnemri T *et al.* The mitochondrial antiviral protein MAVS associates with NLRP3 and regulates its inflammasome activity. *J Immunol* 2013; **191**: 4358–4366.
38. Subramanian N, Natarajan K, Clatworthy MR, Wang Z, Germain RN. The adaptor MAVS promotes NLRP3 mitochondrial localization and inflammasome activation. *Cell* 2013; **153**: 348–361.
39. Martinon F, Petrilli V, Mayor A, Tardivel A, Tschopp J. Gout-associated uric acid crystals activate the NALP3 inflammasome. *Nature* 2006; **440**: 237–241.
40. Mariathasan S, Newton K, Monack DM, Vucic D, French DM, Lee WP *et al.* Differential activation of the inflammasome by caspase-1 adaptors ASC and Ipaf. *Nature* 2004; **430**: 213–218.
41. Kuida K, Lippke JA, Ku G, Harding MW, Livingston DJ, Su MS *et al.* Altered cytokine export and apoptosis in mice deficient in interleukin-1 beta converting enzyme. *Science* 1995; **267**: 2000–2003.
42. Sato T, Stange DE, Ferrante M, Vries RG, Van Es JH, Van den Brink S *et al.* Long-term expansion of epithelial organoids from human colon, adenoma, adenocarcinoma, and Barrett's epithelium. *Gastroenterology* 2011; **141**: 1762–1772.

Supplementary Information accompanies this paper on Cell Death and Differentiation website (http://www.nature.com/cdd)